Plant Physiology®

Kinase regulators evolved into two families by gain and loss of ability to bind plant steroid receptors

Qiang Wei [ID],[1,†] Jing Liu [ID],[1,†] Feimei Guo [ID],[1] Zhuxia Wang [ID],[1] Xinzhen Zhang [ID],[1] Lei Yuan [ID],[1] Khawar Ali [ID],[1] Fanqi Qiang [ID],[1] Yueming Wen [ID],[1] Wenjuan Li [ID],[1] Bowen Zheng [ID],[1] Qunwei Bai [ID],[1] Guishuang Li [ID],[1] Hongyan Ren [ID] [1] and Guang Wu [ID] [1,*]

1   College of Life Sciences, Shaanxi Normal University, Xi'an 710119, Shaanxi Province, P.R. China

*Author for correspondence: gwu3@snnu.edu.cn
†These authors contributed equally to this work.

Abstract

All biological functions evolve by fixing beneficial mutations and removing deleterious ones. Therefore, continuously fixing and removing the same essential function to separately diverge monophyletic gene families sounds improbable. Yet, here we report that brassinosteroid insensitive1 kinase inhibitor1 (BKI1)/membrane-associated kinase regulators (MAKRs) regulating a diverse function evolved into BKI1 and MAKR families from a common ancestor by respectively enhancing and losing ability to bind brassinosteroid receptor brassinosteroid insensitive1 (BRI1). The BKI1 family includes BKI1, MAKR1/BKI1-like (BKL) 1, and BKL2, while the MAKR family contains MAKR2-6. Seedless plants contain only BKL2. In seed plants, MAKR1/BKL1 and MAKR3, duplicates of BKL2, gained and lost the ability to bind BRI1, respectively. In angiosperms, BKL2 lost the ability to bind BRI1 to generate MAKR2, while BKI1 and MAKR6 were duplicates of MAKR1/BKL1 and MAKR3, respectively. In dicots, MAKR4 and MAKR5 were duplicates of MAKR3 and MAKR2, respectively. Importantly, BKI1 localized in the plasma membrane, but BKL2 localized to the nuclei while MAKR1/BKL1 localized throughout the whole cell. Importantly, BKI1 strongly and MAKR1/BKL1 weakly inhibited plant growth, but BKL2 and the MAKR family did not inhibit plant growth. Functional study of the chimeras of their N- and C-termini showed that only the BKI1 family was partially reconstructable, supporting stepwise evolution by a seesaw mechanism between their C- and N-termini to alternately gain an ability to bind and inhibit BRI1, respectively. Nevertheless, the C-terminal BRI1-interacting motif best defines the divergence of BKI1/MAKRs. Therefore, BKI1 and MAKR families evolved by gradually gaining and losing the same function, respectively, extremizing divergent evolution and adding insights into gene (BKI1/MAKR) duplication and divergence.

Introduction

Gene duplication is one of the central mechanisms for generating multigene families with novel functions that might facilitate speciation (Ohno, 1970; Flagel and Wendel, 2009; Magadum et al., 2013; Birchler and Yang, 2022), which includes whole-genome duplication (WGD), tandem and segment duplication, transposon-mediated duplication, and retro-duplication (Magadum et al., 2013; Panchy et al., 2016). Following gene duplication events, duplicates can have different fates (Birchler and Yang, 2022). The most common fate is that one copy retains the original gene function while the other copy is pseudogenized (Lynch and Conery, 2000; Panchy et al., 2016). Alternatively, both duplicates survive long-term, which provides genetic resources for the evolution of functional novelty, namely neofunctionalization (Flagel and Wendel, 2009). Current theoretical models for duplicate retention include the following: (1) gene dosage balance, in which the young duplicates maintain the original function by the correct stoichiometric ratios (Panchy et al., 2016); (2) subfunctionalization, in which two duplicates split the ancestral functions (Hughes, 1994; Force et al., 1999; Rastogi and Liberles, 2005; Panchy et al., 2016); (3) neofunctionalization, in which one copy retains the ancestral function while the other copy acquires a new function by an adaptive process (Innan and Kondrashov, 2010; Panchy et al., 2016). Importantly, neofunctionalization can occur at multiple levels, including gain of novel transcriptional regulation (Hallin and Landry, 2019), relocation of protein subcellular localization (Ren et al., 2014; Qiu et al., 2020; von der Dunk and Snel, 2020), and acquisition of new protein targets (He and Zhang, 2005; Gibson and Goldberg, 2009; Diss et al., 2017). Yet, how the neofunctionalization takes place when the original function is still required remains elusive, which has been called Ohno's dilemma (Bergthorsson et al., 2007).

Receptor-like kinases (RLKs) represent one of the largest families generated by gene duplication and divergence (Shiu and Bleecker, 2001; Gou et al., 2010; Dievart et al., 2020). Brassinosteroid insensitive1 (BRI1), one of the best studied RLKs, perceives brassinosteroids (BRs) by its extracellular domain to activate its downstream signaling pathway through the kinase domain (KD), which regulates almost all aspects of plant growth and development (Li and Chory, 1997). In metazoans, both receptor activation and inhibition are vital for not only receptor signaling but also disease occurrence (Neben et al., 2019). In plants, coreceptor BRI1-associated kinase1 (BAK1) can interact with BRI1 to activate downstream BR signaling cascade (Fabregas et al., 2013). Conversely, BRI1 kinase inhibitor1 (BKI1), coined by Wang and Chory (2006), can interact with BRI1 to inactivate BR signaling (Wang and Chory, 2006; Jiang et al., 2015). In BKI1, the N terminus (NT) is responsible for its plasma membrane (PM) targeting and inhibitory activity, while the C terminus (CT) containing BRI1 interacting motif (BIM) is responsible for its interaction with the BRI1-KD (Jaillais et al., 2011; Wang et al., 2014). Consistently, BKI1 can be phosphorylated by BRI1-KD in vitro and in vivo, hallmarking the active function of BKI1 (Wang and Chory,

2006; Jaillais et al., 2011). As expected, *BKI1*-overexpression lines have a reduced plant stature together with shorter petiole length and rounder rosette leaves compared to the wild types, resembling the weak mutant of *bri1* (Wang and Chory, 2006; Jaillais et al., 2011). Taken together, these results suggest that BKI1 negatively regulates BR signaling by inhibiting BRI1 kinase activity (Wang and Chory, 2006), yet how BKI1 acquires its ability to interact and inhibit BRI1 during evolution is unknown.

In Arabidopsis (*Arabidopsis thaliana*), besides BRI1, there are BRI1-like 1 (BRL1) and BRI1-like 3 (BRL3) that can perceive BRs and rescue the *bri1* mutants, and BRI1-like 2 (BRL2) that cannot (Li and Chory, 1997; Cano-Delgado et al., 2004; Zhou et al., 2004; Kinoshita et al., 2005). Similarly, besides BKI1, there are BKLs, named membrane-associated kinase regulators (MAKRs) identified using the conserved membrane localization motif and the CT (Jaillais et al., 2011). Among these additional *MAKRs*, only MAKR1 can interact with BRI1 and inhibit plant growth when overexpressed in *Arabidopsis*, implying a functional redundancy of MAKR1 and BKI1 (Jaillais et al., 2011). Conversely, MAKR2-6 cannot interact with BRI1 (Jaillais et al., 2011). Instead, MAKR2 directly interacts with the receptor kinase transmembrane kinase1 to regulate the pace of root gravitropism (Marques-Bueno et al., 2021). Furthermore, MAKR4 acts downstream of the IBA-to-IAA conversion pathway, yet its interacting partners have not been identified (Xuan et al., 2015). Additionally, MAKR5 can act downstream of barely any meristem3 (BAM3) and positively regulate the BAM3-dependent CLAVATA3/embryo surrounding region signaling (Kang and Hardtke, 2016). However, no direct interaction of MAKR5 and BAM3 has been reported. Last, the MAKR6 signaling pathway has not been specified, although the expression of *MAKR6* affected by boron and zinc application has been reported in strawberry (*Fragaria x ananassa* Duch) (Kiryakova et al., 2016), leaving only MAKR3 uncharacterized. Nevertheless, all the known MAKRs are important regulators of plant growth and development (Wang and Chory, 2006; Jaillais et al., 2011; Wang et al., 2011, 2017; Jiang et al., 2015; Xuan et al., 2015; Kang and Hardtke, 2016; Marques-Bueno et al., 2021). Therefore, it is imperative to investigate how they derive such a diverse function. However, the evolutionary study of BKI1/MAKRs is still in rudiment (Furumizu and Sawa, 2021; Novikova et al., 2021).

Homologous sequence searches have revealed MAKRs in every land plant lineage, including bryophytes, lycophytes, ferns, gymnosperms, and angiosperms (Bowman et al., 2017; Furumizu and Sawa, 2021; Novikova et al., 2021). One report suggests that the BKI1/MAKRs have two homologous clades in angiosperms, the BKI1/MAKR1/3/4 clade, and MAKR2/5/6 clade (Novikova et al., 2021). In addition, the BKI1/MAKR1/3/4 clade shared one common ancestor in angiosperms, while the MAKR2/5/6 clade diverged into three branches in the common ancestor of angiosperms. Furthermore, there are one to several unclassified MAKRs in gymnosperms and seedless plants (Novikova et al., 2021). However, another study

found both BKI1 and MAKR1 in *Amborella* (*Amborella tricho-poda*) and two distinct types of MAKRs in gymnosperms (Furumizu and Sawa, 2021). Nevertheless, the functional study of BKI1 and MAKRs has not been reported in nonangiosperms. Therefore, in-depth studies are required to clarify the functional evolution of the BKI1/MAKRs in planta. With a large amount of data from the whole genome and transcriptome sequencing available, one can start to explore the origin and evolution of BKI1/MAKRs.

Here, we have performed functional analyses on the selective members of BKI1/MAKRs across land plants and classified BKI1/MAKRs into the BKI1 family that can interact with BRI1 and the MAKR family that cannot interact with BRI1. Interestingly, besides BKI1 and BRI1, there are putatively paralogous BKI1-likes (BKLs) in BKI1 family that are concomitant with BRLs in BRI1 family, respectively (Supplemental Table 1). Namely, BKI1 family comprises BKI1 and BKLs that include BKL1 which has been described as MAKR1 originally coined by Jaillais (Jaillais et al., 2011) and BKL2, another putative MAKR reported in this study, while MAKR family contains MAKR2-6 (Supplemental Table 1). Surprisingly, BKL2 and BRL2, BKL1 and BRL1, and BKI1 and BRI1 co-originated in seedless plants, seed plants, and angiosperms, respectively (Supplemental Table 1). Importantly, we show that BKI1 strongly and MAKR1/BKL1 weakly inhibit plant growth, while BKL2 and other MAKRs do not. Since seedless plants have only BKL2 but not any other putative MAKR orthologs, BKI1, MAKR1/BKL1, and other MAKRs derive in seed plants and angiosperms from a common ancestor shared with BKL2 in the common ancestor of land plants. As such, MAKR1/BKL1, BKL2, and MAKR3 are present in gymnosperms, implying a gain of the inhibitory function in MAKR1/BKL1 and a loss of the interactive function in MAKR3 after duplication events in seed plants (Supplemental Table 1). Surprisingly, angiosperms have BKI1, MAKR1/BKL1, and MAKR2 with the absence of BKL2, implying a further gain of the additional inhibitory function in BKI1 after another duplication event and the loss of the interactive function in BKL2 to generate MAKR2 in angiosperms (Supplemental Table 1). In addition, MAKR3 was duplicated to generate MAKR6 in angiosperms. Finally, MAKR3 and MAKR2 were further duplicated to generate MAKR4 and MAKR5 in dicots, respectively (Supplemental Table 1). Taken together, BKI1/MAKRs evolved into BKI1 family by gradually improving the ability to bind BRI1 and gaining the ability to inhibit BRI1, and MAKR family by gradually losing the ability to bind BRI1 from a common ancestor that is only able to bind BRI1 during land plant evolution.

Results

Classifying angiosperm BKI1/MAKRs by BIMs

Previous studies suggest that BKI1/MAKRs play an important role in regulating a diverse range of biological functions. To determine how BKI1/MAKRs derive such a diverse function, we performed a phylogenetic analysis, followed by functional characterization and evolutionary reconstruction. To do so, we first retrieved the protein sequences of BKI1 and MAKRs from *Arabidopsis* (downloaded from TAIR) and then used them as queries to search Phytozome V13.0 (https://phytozome.jgi.doe.gov), Plantgenie (https://plantgenie.org/), (GIGA)^{n}DB, and NCBI (https://www.ncbi.nlm.nih.gov/) for their respective homologs in the other species using the BLASTp algorithm (Sneddon et al., 2012). We next downloaded BKI1/MAKR homologs from PhyloGenes (Zhang, Berardini, et al., 2020; Zhang, Chen, et al., 2020). We finally confirmed their homology by manually comparing their conserved BIMs (Supplemental Figure 1A and Supplemental Dataset 1). Specifically, we first analyzed angiosperm BKI1/MAKRs and then examined gymnosperm BKI1/MAKRs. We then investigated seedless plant BKI1/MAKRs and finally explored the underlying mechanism of the functional evolution of BKI1/MAKRs.

To study BKI1/MAKRs in angiosperms, we constructed a phylogenetic tree by the maximum-likelihood (ML) method using the BIM that hallmarks BKI1/MAKRs (Jaillais et al., 2011; Wang et al., 2014). The phylogenetic tree was resolved into three major clades (Figure 1). BKI1 and MAKR1/BKL1 were clustered into one clade sister to both MAKR3/4/6 and MAKR2/5 clades (Figure 1 and Supplemental Dataset 2). Surprisingly, the tree topology differs from the previous report (Novikova et al., 2021). Interestingly, the phylogenetic trees of the full-length and the NT of BKI1/MAKRs showed a distinct topology by relocating MAKR6 such that MAKR6 and MAKR2/5 located in a branch sister to both MAKR1/BKL1 and MAKR3/4 (Supplemental Figures 2 and 3 and Supplemental Datasets 3 and 4), creating an uncertainty that required further investigation. Nevertheless, our analysis suggests that MAKR5 is probably less divergent from BKI1/MAKR1, consistent with a report that the NT of MAKR5 is replaceable by that of BKI1 (Figure 1 and Supplemental Figures 2 and 3) (Kang and Hardtke, 2016).

MAKR2-6 lose the ability to inhibit plant growth via BRI1

We confirmed that the overexpression of *MAKR1/BKL1* inhibited much less plant growth than that of *BKI1* under the control of four different promoters (Supplemental Figure 4), clearly implying that BKI1 is functionally stronger than MAKR1/BKL1. This was validated by transcriptional down-regulation of BR biosynthesis genes *CONSTITUTIVE PHOTOMORPHOGENIC DWARF* (*CPD*), and *DWARF4* (*DWF4*) and up-regulation of BR metabolic gene *PHYB ACTIVATION-TAGGED SUPPRESSOR1* (*BAS1*) and *SMALL AUXIN UP RNA* (*Saur-AC1*) with or without the treatment of eBL (24-epi-BR) (Supplemental Figure 5, A–C) (Wang and Chory, 2006). In addition, we detected less responsiveness of dephosphorylation of BRI1-ethylmethanesulfonate (EMS)-suppressor1 (BES1), an activation marker of BR signaling, with the treatment of eBL in *MAKR1/BKL1* and *BKI1* overexpression lines (Supplemental Figure 5D). Taken
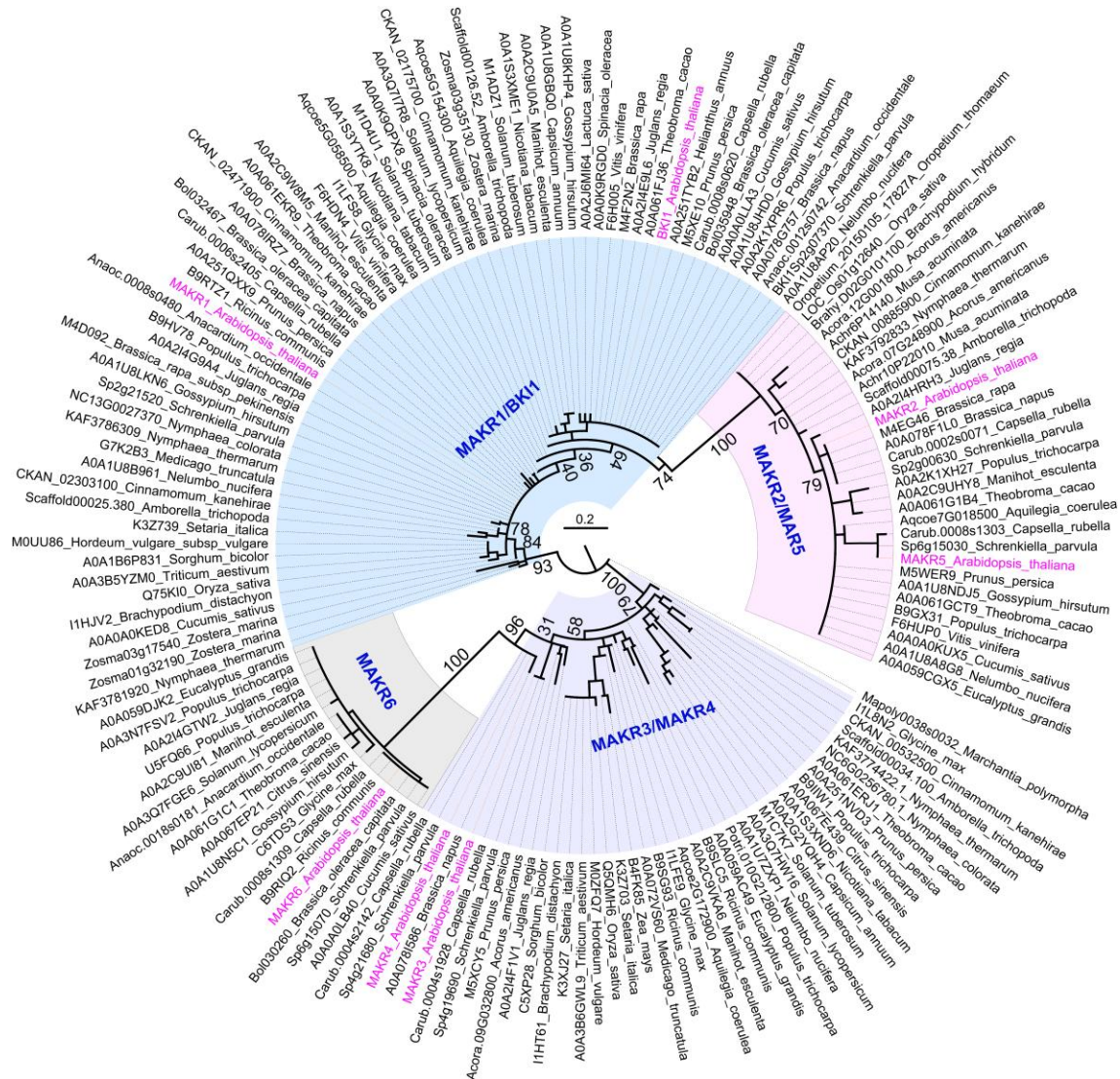
Figure 1 Phylogeny of BKI1/MAKR homologs in angiosperms. The BIM was used to build the ML tree using IQ-TREE (it is the successor of IQPNNI and TREE-PUZZLE software) under the JTTDCMut (the "Direct Computation with Mutabilities" [DCMut] versions of JTT) + G4 model. The BKI1/MAKR in *Marchantia polymorpha* was used as the outgroup. Support values were obtained from 1,000 bootstrap replicates and displayed on the major branches. The scale bar indicates 0.2 substitutions per site. Pink letters indicate the BKI1/MAKRs from Arabidopsis for functional analysis. Please refer to Supplemental Dataset 2 for the detailed bootstrap values and aligned sequences.

together, these results confirm that MAKR1/BKL1, like BKI1, is involved in BR signaling (Jaillais et al., 2011).

On the other hand, MAKR2-6 did not interact with BRI1, and neither did the CT of MAKR2/5 (Figure 2, A–C). As expected, we confirmed that the overexpression of *MAKR2-6* under the *BRI1* promoter did not inhibit plant growth (Figure 2, D and E). These results imply that *MAKR2-6* do not function through BR receptors (Jaillais et al., 2011; Kang and Hardtke, 2016; Marques-Bueno et al., 2021). Interestingly, *MAKR3*-overexpression lines had larger leaves with rounder leaf shapes and larger angles between lateral branches and main stems as well as between petiole and lateral branches (Figure 2, D–G). We then tried to determine the domain responsible for this specific phenotype by

swapping the NT or CT between BKI1 and MAKR3 (Supplemental Figure 6A). We found that MAKR3-BKI1 (the NT of MAKR3 [1–274] fused to the CT of BKI1 [304–337]) interacted with BRI1 (Supplemental Figure 6, A and B). Yet, *MAKR3-BKI1* overexpression lines under the control of the *MAKR3* promoter lost the phenotypes shown in both *MAKR3* and *BKI1* overexpression lines (Supplemental Figure 6, C and D). Conversely, the complementary construct BKI1-MAKR3 (the NT of BKI1 [1–303] fused to the CT of MAKR3 [275–321]) lost its interaction with BRI1 (Supplemental Figure 6B). Furthermore, overexpression of *BKI1-MAKR3* lost the phenotypes shown in the overexpression lines of either *MAKR3* or *BKI1* (Supplemental Figure 6, C and D). These results suggest that *BKI1* and *MAKR3* have

Figure 2 MAKR2–6 lose the ability to inhibit plant growth via BRI1. A, Schematic representation of MAKRs used for experi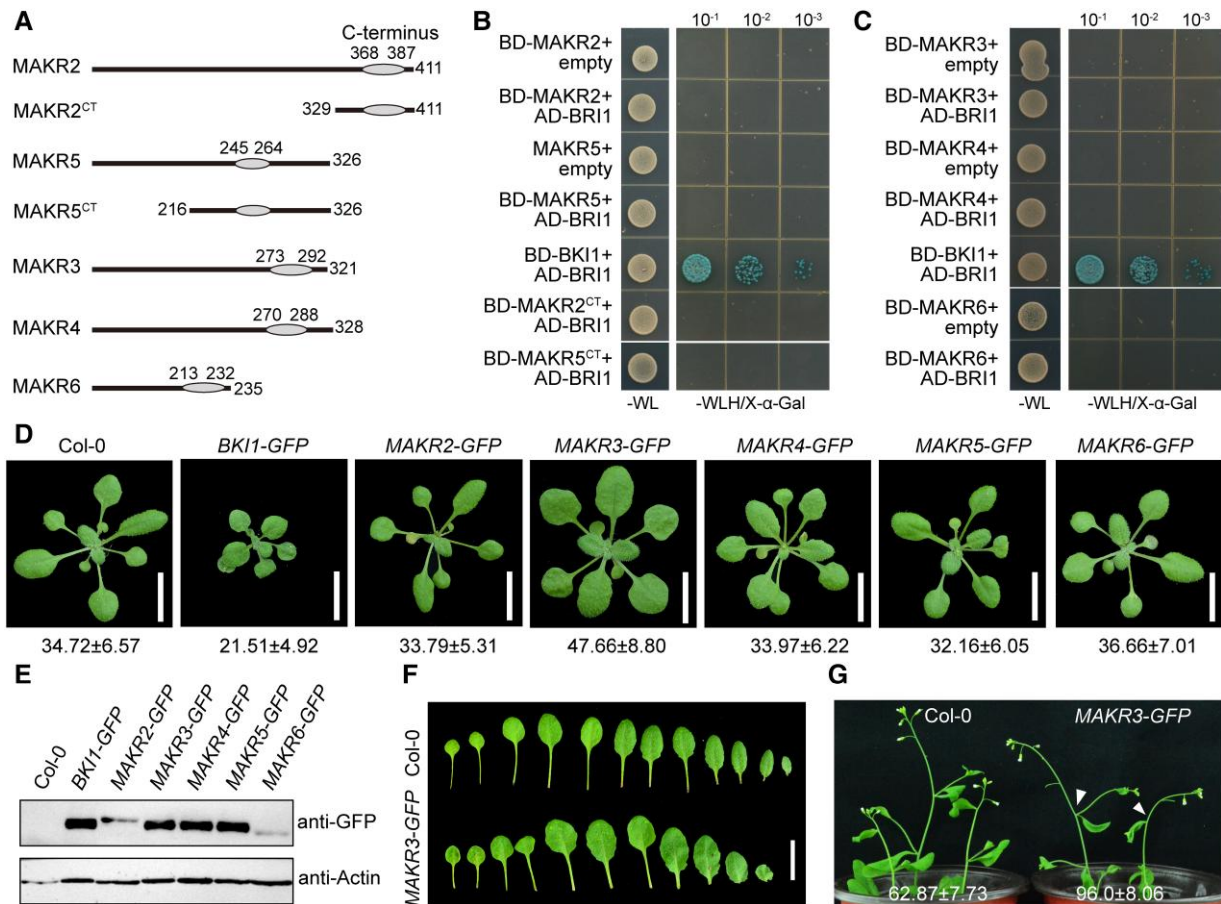ments. B and C, Interactions of MAKRs with BRI1 in yeast cells. BKI1 interaction with BRI1 was used as a positive control. D, Phenotypes of transgenic plants over-expressing *MAKRs* driven by *BRI1* promoter. The *BKI1*-overexpression line was used as a reference for the inhibitory phenotype. Scale bars, 1 cm. Images were digitally extracted for comparison. Leaf area in square millimeters ± SD (mean ± SD) (*n* ≥ 10 plants). E, The protein expression levels of transgenic plants as shown in (D). F, Phenotypic comparison of rosette leaves between Col-0 and *MAKR3-GFP* overexpression lines. GFP, green fluorescent protein. Scale bar, 1 cm. G, Phenotypes of 5-week-old transgenic plants overexpressing *MAKR3* and wild type. White arrows indicated the large angle between the lateral branch and the main stem compared with Col-0. Numbers indicate angle (mean ± SD) (*n* = 10 plants).

drastically functional divergence in both their NTs and CTs. Taken together, angiosperm MAKRs can be classified into two groups, one that can interact with BRI1 and one that cannot. Yet, the MAKRs from gymnosperms and seedless plants have not been fully studied (Novikova et al., 2021).

Presence of BKL2 but absence of MAKR2/5 in gymnosperms

To study MAKRs from gymnosperms, we constructed the phylogenetic tree of MAKRs from land plants (Figure 3; Supplemental Figures 1, 7, 8 and Supplemental Datasets 5–7). We found gymnosperm MAKRs in three distinct branches, with one sister to both angiosperm BKI1 and MAKR1/BKL1, another sister to angiosperm MAKR3/4, and the last sister to angiosperm MAKR2/5 (Figure 3). Identity analysis showed that MAKR1/BKL1 from *Arabidopsis* and *Amborella* shared 25.7%–29.1% sequence identity with the homologs from Norway spruce (*Picea abies* [Pa],

MA_52346g0010) and Ginkgo (*Ginkgo biloba*, Gb_04579). In contrast, BKI1 shared only 16.6%–19.8% identities with these homologs (Supplemental Table 2 and Supplemental Dataset 8), consistent with previous reports that no ortholog of BKI1 was found in gymnosperms (Wang and Chory, 2006; Wang et al., 2021). We thus named them gymnosperm BKL (gBKL1). We further uncovered that PaBKL1 (MA_52346g0010, BKL1 in Pa) could interact with and be transphosphorylated by BRI1 in Y2H and in vitro phosphorylation assays, respectively (Figure 4, A and B). Importantly, the overexpression of *PaBKL1* under the *BRI1* promoter inhibited plant growth less than that of *BKI1* but more than that of *MAKR1/BKL1*, consistent with our evolutionary analysis (Figure 4, C–E and Supplemental Figure 5, A–D). Therefore, we place PaBKL1 as an evolutionary intermediate sister to both angiosperm BKI1 and MAKR1/BKL1 (Figure 3).

Besides PaBKL1, there was a branch of gymnosperm MAKRs sister to both PaBKL1 and angiosperm MAKR2/5 (Supplemental Figure 7). Noticeably, there were eight copies
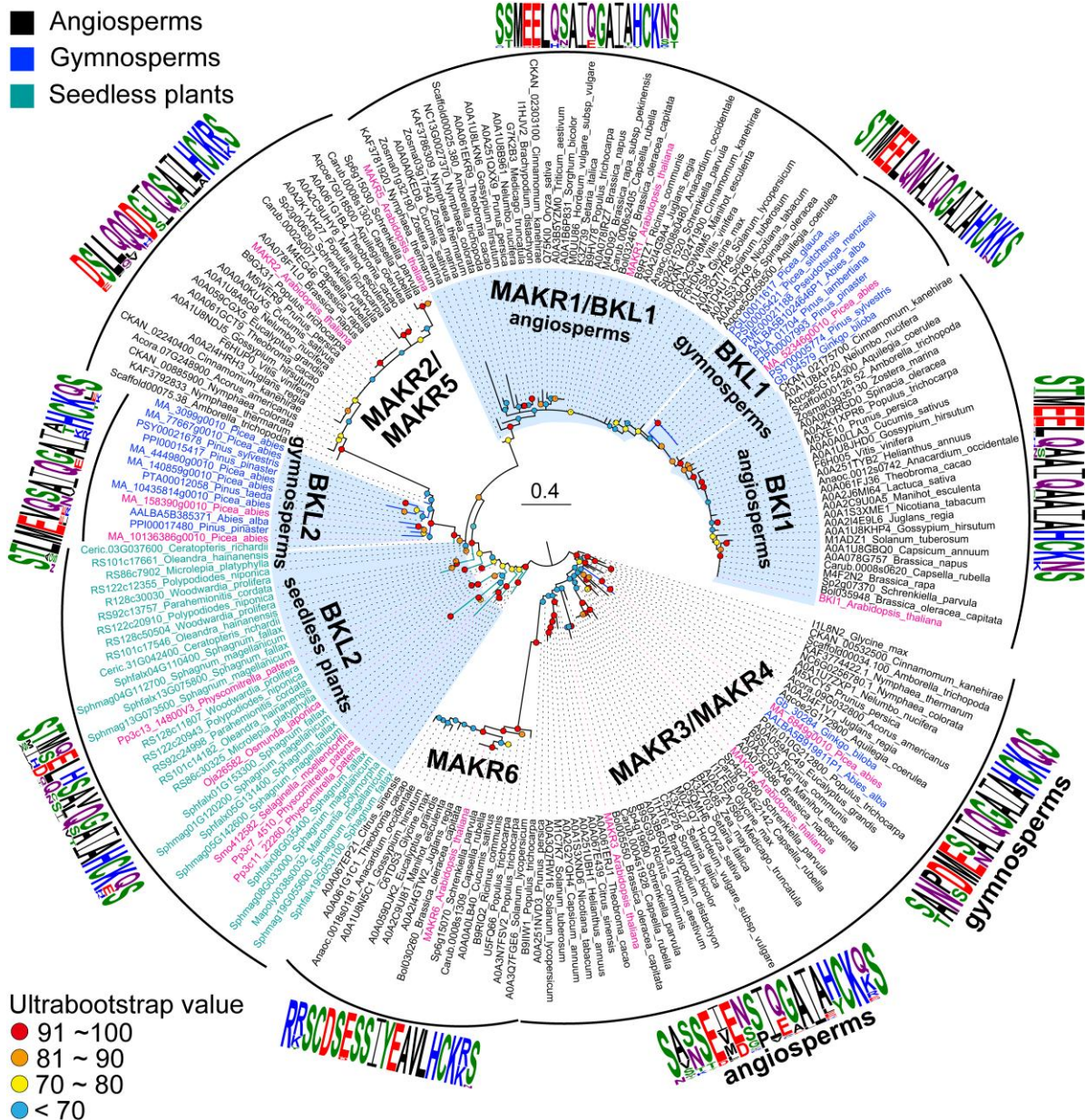
Figure 3 Phylogenetic relationships of BKI1/MAKRs from land plants. We performed a ML analysis in IQ_TREE using the BIM of BKI1/MAKR homologs with 1,000 ultrafast-bootstrap replicates. The best-fit substitution model, JTT + G4, was detected using automatic model selection based on the Bayesian information criterion in IQ_TREE. The 244 amino acid sequences from 65 land plant species were aligned using the MAFFT program. The discs of different colors label the bootstrap support (based on 1,000 replicates) for each node: red (91–100), orange (81–90), yellow (70–80), and blue (below 70). The scale indicates a mutation rate of 0.4 substitutions per site. Pink letters indicate BKI1/MAKRs from the representative species used for functional analysis. Blue and aquamarine letters indicate BKI1/MAKRs in gymnosperms and seedless plants, respectively. Sequence logos illustrate the conserved amino acid motifs in the BKI1/MAKRs within each branch. Please refer to Supplemental Dataset 5 for the detailed bootstrap values and aligned sequences.

of this type of MAKRs in Pa, two in *Cycas panzhihuaensis*, but none in *Ginkgo biloba*, which means that *Ginkgo biloba* might lose this type of homolog and that this type of MAKRs is not essential in gymnosperms (Supplemental Figure 9) (Nystedt et al., 2013; Liu et al., 2021, 2022). Yet, there are eight copies of these gymnosperm MAKRs that shared 48%–85% sequence identities among themselves, but only 18%–22%

sequence identities with PaBKL1 in Pa (Supplemental Figure 10 and Supplemental Table 3), suggesting that they are duplicates putatively paralogous to PaBKL1.

We then used two of them (MA_158390g0010 and MA_10136386g0010) as representatives to examine their ability to interact with BRI1 (Supplemental Figure 10). We observed that both of them interacted with BRI1 in Y2H
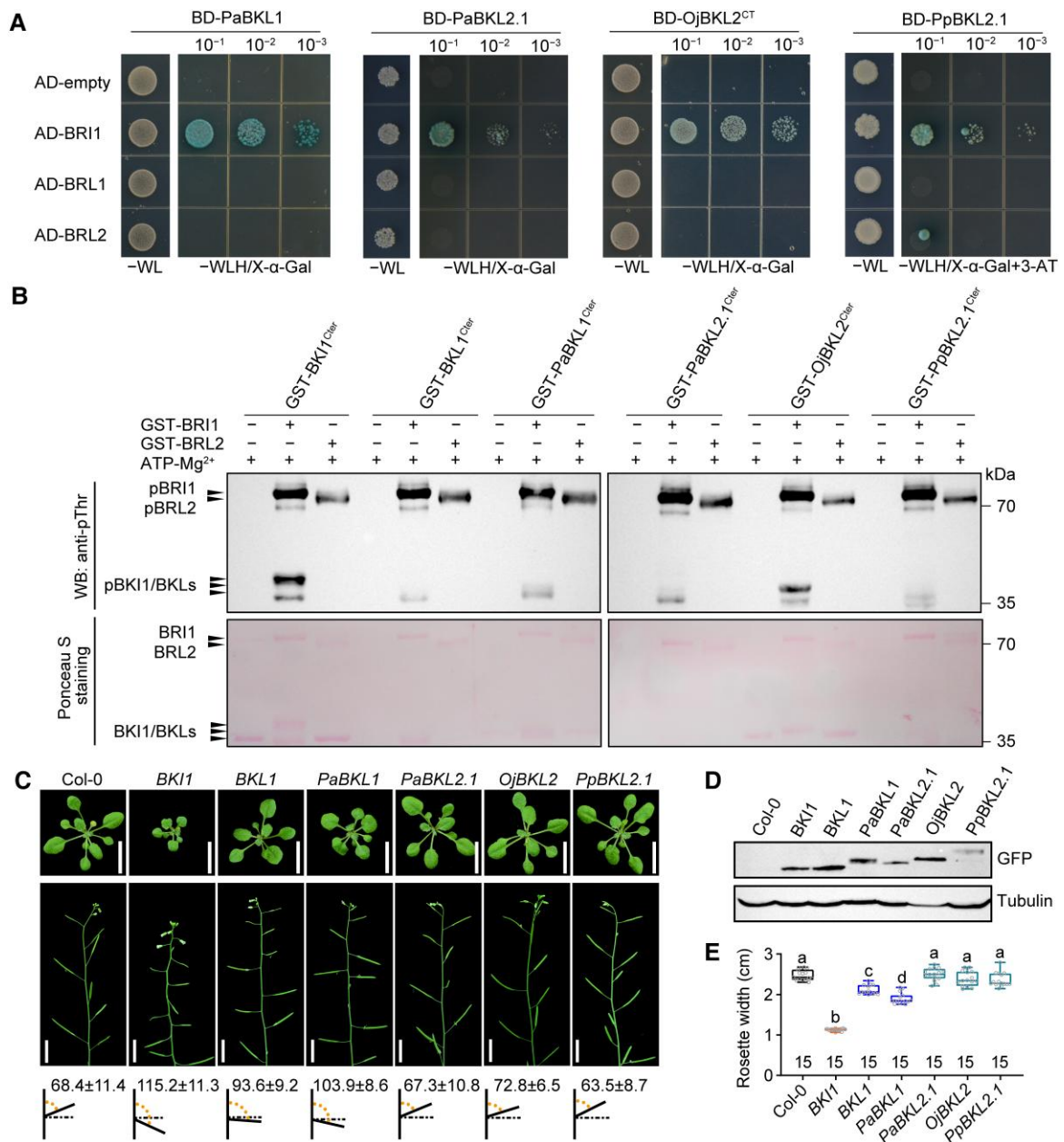
Figure 4 Functional divergence in BKI1 family. A, Yeast two-hybrid assays showing the interactions of BR receptors with BKLs in representative species. The CT of OjBKL2 was used because of the autoactivation of the full-length protein. PaBKL2.1, one copy of BKL2 in Pa; PpBKL2.1, one copy of BKL2 in Pp; B, In vitro transphosphorylation of BKI1 family members by the BRI1 KD. The KD of BRL2 was used as a negative control. Ponceau S staining determined protein transfer efficiency, and the phosphorylation level was detected by immunoblotting with Phospho-Threonine Antibody. Cter, C-terminal domain as shown in Supplemental Figure 12. C, Rosette leaves and inflorescence architecture of Col-0 and the transgenic plants under the *BRI1* promoter. The lower panel displayed the average pedicel angles $\pm$ SD (mean $\pm$ SD) ($n \geq 15$). Scale bars, 1 cm. All images were digitally extracted for comparison. D, Abundance of proteins was quantified by immunoblot with an anti-GFP antibody. Tubulin was used as the loading control. E, Measurements of rosette width of plants from (C) ($n = 15$). Boxplots show the first quartile (lower), median, and third quartile (upper). Whiskers show the full data range. Different letters indicate significant differences ($P < 0.05$) by one-way ANOVA and Tukey's multiple comparisons test.

(Figure 4A and Supplemental Figure 11A). We further used one representative (*MA_158390g0010*) to assess its ability to be transphosphorylated by BRI1. We found that it was transphosphorylated by BRI1 at a level similar to that of PaBKL1 (Figure 4B and Supplemental Figure 12). We last

overexpressed this copy in Col-0 to test its inhibitory effect and found that it failed to inhibit plant growth (Figure 4, C–E and Supplemental Figure 11, B–D). Therefore, this type of MAKRs was named gBKL2 rather than gymnosperm MAKR2/5, although gBKL2 and MAKR2/MAKR5 might arise

from a common ancestor (Figure 3 and Supplemental Figure 7). With a recent report showing that MAKR5^{NT} is replaceable by BKI1^{NT}, MAKR2/MAKR5 could be additional members of MAKR family derived from BKI1 family in angiosperms. However, gBKL2 retained the ability to interact with BRI1, but MAKR2/MAKR5 did not. One possibility is that MAKR2/MAKR5 is a loss-of-function mutant of BKL2. In this scenario, gBKL2 can be placed as an evolutionary intermediate of MAKR1/BKL1 and MAKR2/MAKR5 (Supplemental Figure 7). On the other hand, a gymnosperm MAKR sister to angiosperm MAKR3/4 did not interact with BRI1 (Supplemental Figure 13), consistent with the idea that they are a putative ortholog of MAKR3/4 in gymnosperms. We thus named it gMAKR3 (gymnosperm MAKR3). Together, we uncover MAKR1/BKL1, BKL2, and MAKR3 but not BKI1 or MAKR2/5 in gymnosperms, in which gBKL1 and gBKL2 are able to interact with BRI1, but gMAKR3 is unable to interact with BRI1 (Figure 4 and Supplemental Figures 9 and 13).

Presence of only BKL2 in seedless plants

We last studied BKI1/MAKRs in seedless plants and found them clustered into one clade sister to all known BKI1/MAKRs in seed plants (Figure 3 and Supplemental Figure 7). We then chose three representatives to test whether they could interact with BRI1 and showed that the MAKRs from *Osmunda japonica* (Oj) (ferns), *Selaginella moellendorffii* (lycophytes), and *Physcomitrium patens* (Pp) (mosses) did interact with BRI1 in Y2H (Figure 4A and Supplemental Figure 11A). Further, they were transphosphorylated by BRI1 in vitro (Figure 4B and Supplemental Figure 12). However, overexpression of them failed to inhibit plant growth and BR response (Figure 4, C–E and Supplemental Figure 11, B–D) functionally resembled PaBKL2. Since all these MAKRs were sister to the common ancestor of the BKI1/BKL1/BKL2 clade in seed plants, here we named them BKL2.

In contrast to land plants, no MAKRs existed in algae (Supplemental Figure 9A). Therefore, MAKRs originate in the common ancestor of land plants after they diverge from algae. The ancestral MAKRs then diverge into the BKI1 family that is able to bind and inhibit BRI1, and MAKR family that is unable to bind BRI1 from a common ancestor sister to BKL2 that is only able to bind BRI1. It is conceivable that BKI1 family includes BKL2, MAKR1/BKL1 and BKI1 emerged in land plants, seed plants and angiosperms, respectively, implying a functional gain in BKI1 family. On the other hand, MAKR family includes MAKR3, MAKR6 together with MAKR2, and MAKR5 together with MAKR4 emerged in seed plants, angiosperms and dicots, respectively (Supplemental Figure 9). As such, MAKR6 is a duplicate of MAKR3 in angiosperms, while MAKR4 is a duplicate of MAKR3 in dicots. In addition, MAKR2 might be a loss-of-function mutant of BKL2 in angiosperms, while MAKR5 is a duplicate of MAKR2 in dicots. As a result, BKI1 family evolves into BKI1, MAKR1/BKL1, and BKL2 during

the land plant evolution, likely improving the preexistent ability to interact with BRI1 and acquiring the new ability to inhibit BRI1 in BKI1 and MAKR1/BKL1. Conversely, five members of the MAKR family are derived by a loss of the ability to interact with BRI1 after duplication events in seed plants (Figure 2 and Supplemental Figure 9), thus gaining new functions independent of BRI1 signaling after gene duplication.

Neofunctionalization of the NT of the BKI1 family

Although BKL2 interacted with BRI1 and was transphosphorylated by BRI1, it did not inhibit plant growth (Figure 4 and Supplemental Figure 11), implying a lack of inhibitory function in BKL2. To find the cause, we replaced the BKI1^{NT} with the BKL2^{NT} from Pa, Oj, and Pp in BKI1 and expressed them in Arabidopsis (Supplemental Figures 14 and 15). All transgenic plants overexpressing these chimeras were indistinguishable from wild-type plants (Figure 5, A and B). In contrast, when we expressed the chimeras of the BKI1^{NT} with the CT of a variety of BKL2 in Arabidopsis, they all inhibited the transgenic plant growth compared to the wild-type plants (Figure 5, A and B and Supplemental Figure 14). Similarly, dark-induced hypocotyl elongation was inhibited as well (Figure 5, C and D). Taken together, in BKI1 family, the CT is responsible for the ability to interact with BRI1, while the NT is responsible for the ability to inhibit plant growth through an association with BRI1.

BKI1 must be anchored to the PM to regulate BR signaling (Jaillais et al., 2011). We observed that BKI1 localized to the PM, whereas MAKR1/BKL1 localized to PM, cytoplasm, and nucleus. However, we could not detect the PM localization of BKL2 in root cells. Instead, BKL2 was almost exclusively localized to the nucleus (Figure 5E), suggesting that BKI1/BKL1 might acquire the PM localization during evolution. We further found that BKL2^{NT} chimeric with BKI1^{CT} still localized to the nucleus (Figure 5E), implying a cause of the lack of PM localization in BKL2^{NT}. We then tested whether the lack of PM localization in BKL2^{NT} was the only cause that led to the loss of the ability to inhibit plant growth. We thus tethered PaBKL2 and OjBKL2 to the PM by adding an NT myristoylation site (MGICMSR) (Wang and Chory, 2006). Surprisingly, the transgenic plants were found to remain indistinguishable from the wild-type plants, albeit that the two variants of myristoylated BKL2 were actually localized to PM (Figure 5, F and G). Together, these results suggest that multiple mechanisms are required for the neofunctionalization of the NT in BKI1 family to acquire an inhibitory function to BR receptors during evolution.

A gain of function in the NT and CT of the BKI1 family

The neofunctionalization model hypothesizes that the ancestral function is retained in the original duplicate by stronger purifying selection, while the extra duplicate neofunctionalizes by relaxation of selective constraint, followed by fixation of the beneficial mutations (Ohno, 1970). In this model, there is a big problem in how the extra duplicate can survive in the
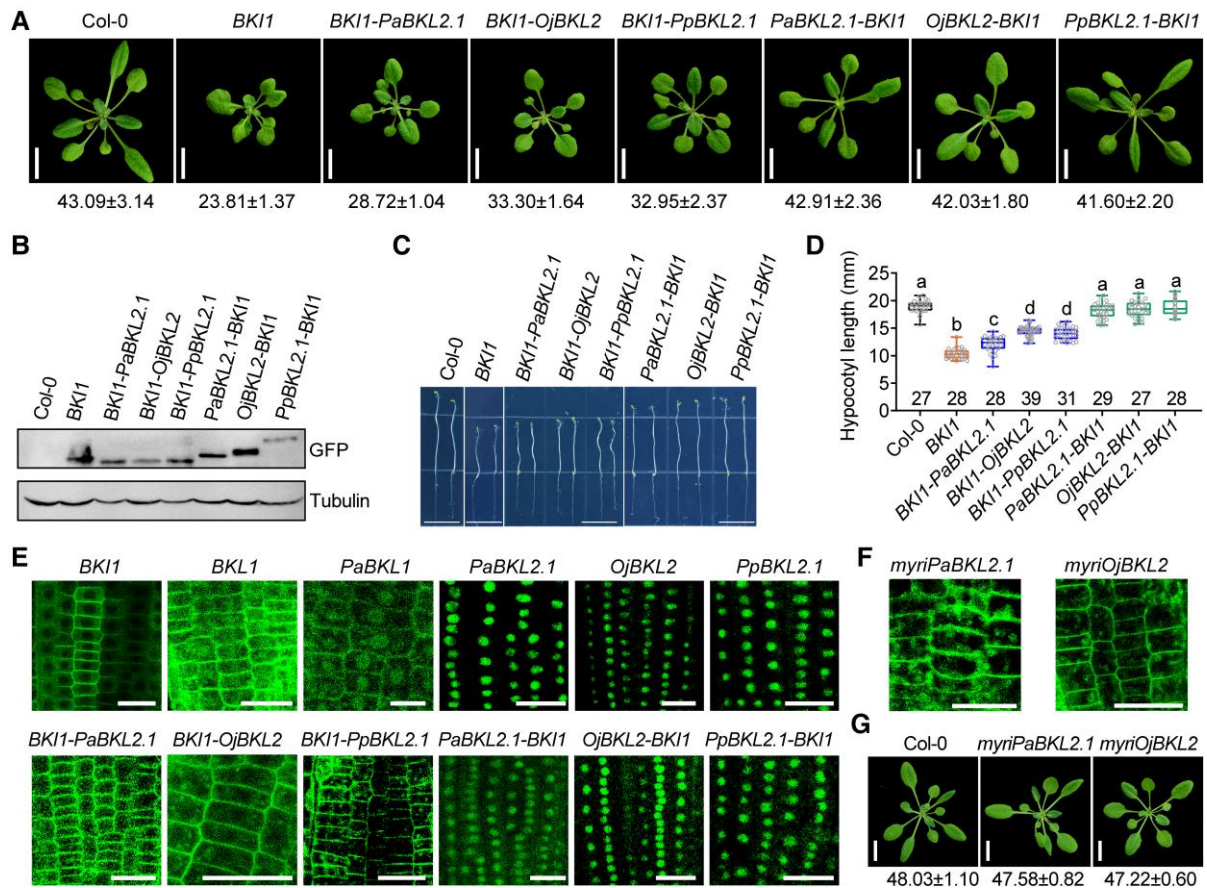
Figure 5 Neofunctionalization of the NT of the BKI1 family. A, Phenotypes of 4-week-old Col-0 and transgenic plants expressing *BKI1* and its chimeras driven by the *BRI1* promoter in Col-0. Scale bars, 1 cm. Rosette diameter in millimeters ± SD (*n* = 15) was shown. B, Protein levels were quantified by immunoblot with an anti-GFP antibody. Tubulin was used as the loading control. C, Morphologies of 5 days dark-grown seedlings on ½ MS plate. Scale bars, 1 cm. D, Comparison of hypocotyl lengths of seedlings from (C). Numbers represent independent plants of every genotype from two different ½ MS plates. Boxplots show the median, and lower (first) and upper (third) quartiles. Whiskers show the full data range. Different letters indicate significant differences (*P* < 0.05) by one-way ANOVA and Tukey's multiple comparisons test. E, Representative confocal images of wild-type and chimeric genes. Scale bars, 25 μm. F, Subcellular localization of genes with myristoylation signal. Scale bars, 25 μm. G, Phenotypes of transgenic plants over-expressing BKL2 with myristoylation signal. Rosette diameter in millimeters ± SD (*n* = 10) was shown. Scale bar, 1 cm. Images in (A), (C), and (G) were digitally extracted for comparison.

relaxation stage since it must face a constant challenge from the accumulation of a large number of deleterious and neutral mutations with only rare beneficial mutations in a long enough time before the new functions arise, which is so-called Ohno's dilemma (Bergthorsson et al., 2007). Nevertheless, this model suggests that the original duplicate should be more conserved than the extra duplicate during evolution.

Our above study clearly suggests that MAKR1/BKL1 is a duplicate of BKL2 in seed plants, and the NT of MAKR1/BKL1 (and BKI1) have acquired an ability to inhibit plant growth via their ability to bind BRI1 through their CT (Figures 4 and 5 and Supplemental Figure 4). Since there is no BKL2 in angiosperms, we can only compare the sequence identity of MAKR1/BKL1 and BKI1 from angiosperms to further understand how BKI1 family evolves. To remove a sampling error and sequence bias, we only used the sequences

from the angiosperm species that have both BKI1 and MAKR1/BKL1 (*n* = 42). We obtained an identity of every pair of putative orthologs, followed by their average to attain the average pairwise identity of BKI1 and MAKR1/BKL1, respectively. We showed that the average pairwise identity in putative orthologs of MAKR1/BKL1 (43%) was much higher than that of BKI1 (34%), consistent with the idea that MAKR1/BKL1 is the original duplicate with less divergence while BKI1 is the extra duplicate with more divergence after duplication in angiosperms (Figure 6A and Supplemental Dataset 8). However, BKI1 had higher ability to interact and inhibit BRI1 (inhibit plant growth via BRI1), higher transphosphorylatability by BRI1, and more exclusive PM localization than that of MAKR1/BKL1 (Figures 4B and 5E and Supplemental Figure 5) (Wang and Chory, 2006; Jaillais et al., 2011), clearly suggesting a gain of function in BKI1 relative to MAKR1/BKL1. Further analysis revealed that the
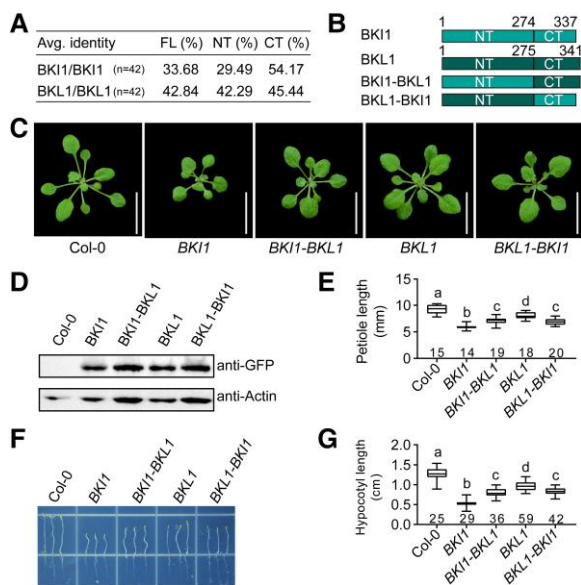
Figure 6 A gain of function in the NT and CT of the BKI1 family. A, Percentage of protein sequence identity within putatively orthologous protein pairs. In total, 42 species with both BKI1 and BKL1 were used. Numbers indicated the average identity for pairwise comparisons. The sequences are provided in Supplemental Dataset 8. B, Schematic overview of the reciprocal replacement of NT and CT between BKI1 and BKL1. Numbers indicated the amino acid position. C, Phenotypes of Col-0 and transgenic plants. Scale bars, 1 cm. Images were digitally extracted for comparison. D, Protein levels were quantified by immunoblot with an anti-GFP antibody. Actin was used as the loading control. E, Comparison of petiole lengths of plants as shown in (C). F, Morphologies of five days dark-grown seedlings on ½ MS plate. G, Comparison of hypocotyl lengths of seedlings from (F). Numbers represent independent plants of every genotype from two different ½ MS plates. In (E) and (G), boxplots show the median, and lower (first) and upper (third) quartiles. Whiskers show the full data range. Different letters indicate significant differences ($P < 0.05$) by one-way ANOVA and Tukey's multiple comparisons test. FL, full-length protein sequence.

$BKI1^{NT}$ had only 29% average pairwise identity, much lower than $BKL1^{NT}$ that had 42% average pairwise identity (Figure 6A). Conversely, the $BKI1^{CT}$ had 54% average pairwise identity much higher than $BKL1^{CT}$ that had only 45% average pairwise identity (Figure 6A). Altogether, these data reveal higher selective constraint in $BKL1^{NT}$ than in $BKI1^{NT}$, consistent with the neofunctionalization model in which the extra duplicate evolves by either relaxation of selective constraint or positive selection. If $BKI1^{NT}$ has a stronger function than $BKL1^{NT}$, $BKI1^{NT}$ evolves by positive selection; but if $BKI1^{NT}$ has a weaker function than $BKL1^{NT}$, $BKI1^{NT}$ evolves by relaxation of selective constraint (neutral selection). Hence, we conclude that $BKI1^{NT}$ evolves by positive selection. On the other hand, our data suggest a higher selective constraint in $BKI1^{CT}$ than in $BKL1^{CT}$, implying a possible relaxation of selective constraint in $BKL1^{CT}$ if $BKL1^{CT}$ has a weaker function than $BKI1^{CT}$. Indeed, the expression of *BKI1-BKL1* or *BKL1-BKI1* had an intermediate inhibitory phenotype

compared to that of *BKI1* and *MAKR1/BKL1* (Figure 6, B–G). These results support that both $BKI1^{NT}$ and $BKI1^{CT}$ have a stronger function than $BKL1^{NT}$ and $BKL1^{CT}$, respectively. Therefore, we reveal positive selection in the $BKI1^{NT}$ and purifying selection in the $BKI1^{CT}$ (implying relaxation of selective constraint in $BKL1^{CT}$) during the neofunctionalization of BKI1 after gene duplication (Jiang et al., 2015).

Coevolution of BKI1 and BRI1 families in planta
MAKRs are identified by the presence of BIM and a reiterated [KR][KR] membrane targeting motif (Jaillais et al., 2011; Wang et al., 2014). The [KR] (179–180) [KR] (197–198) motif is required for the PM localization of Arabidopsis BKI1 (Supplemental Figure 15) (Jaillais et al., 2011). Interestingly, although we did find [KR][KR] in all MAKRs, the numbers and locations of [KR] in the MAKRs are not conserved (Jaillais et al., 2011) (Supplemental Figure 15) (Jaillais et al., 2011). For instance, PaBKL1 had 3 [KR], while OjBKL2 had 7 [KR] (Supplemental Figure 15). Yet, PaBKL1 was partially localized to the PM, while BKL2 putative orthologs that had 3-7 [KR] were localized to the nucleus. In addition, PaBKL1 could inhibit plant growth but BKL2 putative orthologs did not (Figure 4, C–E). Nevertheless, BKL2 and all MAKR1/BKL1 had an ability to interact with BRI1, while MAKR2-6 did not. As such, BIM is highly conserved in sequences but diverged in functions of BKI1/MAKRs. Therefore, BIM best defines BKI1/MAKRs (Figures 1 and 2).

Our finding clearly suggests that BKI1/MAKRs can be classified into two families, in which BKI1 family has an ability to interact with BRI1 (family), while MAKR family has no such ability (Figures 1 and 2 and 7A). The question is whether BRI1 and BKI1 families coevolve during plant evolution. Having a similar evolutionary history is an indication of coevolution (de Juan et al., 2013). We found that both BRL2 and BKL2 first appeared in early land plants, while both BRL1 and MAKR1/BKL1 first presented in seed plants. Furthermore, both BRI1 and BKI1 only existed in early flowering plants (Supplemental Tables 1 and 4), suggesting that BRI1 and BKI1 families share an evolutionary history.

BRI1 and BRLs contain leucine-rich repeats (LRRs) and a 70-amino acid hormone-binding island domain (ID) (Li and Chory, 1997; Wang et al., 2001; Cano-Delgado et al., 2004; Kinoshita et al., 2005). The ID and its neighboring LRRs form BR-binding domain (BD) that is necessary and sufficient for BR perception (Kinoshita et al., 2005; Wang et al., 2021). Hence, BD best characterizes BRI1 family, while BIM best defines BKI1/MAKRs (Li and Chory, 1997; Wang et al., 2001; Cano-Delgado et al., 2004; Kinoshita et al., 2005). Therefore, BIM and BD can best represent the evolution of BKI1 and BRI1 families, respectively.

Sharing phylogenetic trees (mirrortree) is another indication of coevolution (de Juan et al., 2013; Ochoa et al., 2015). Representing by the phylogenetic trees of BIM and BD from selective members of BKI1 family and BRI1 family, respectively, the phylogenetic tree of BKI1 family mirrored the phylogenetic tree of BRI1 family (Figure 7A and
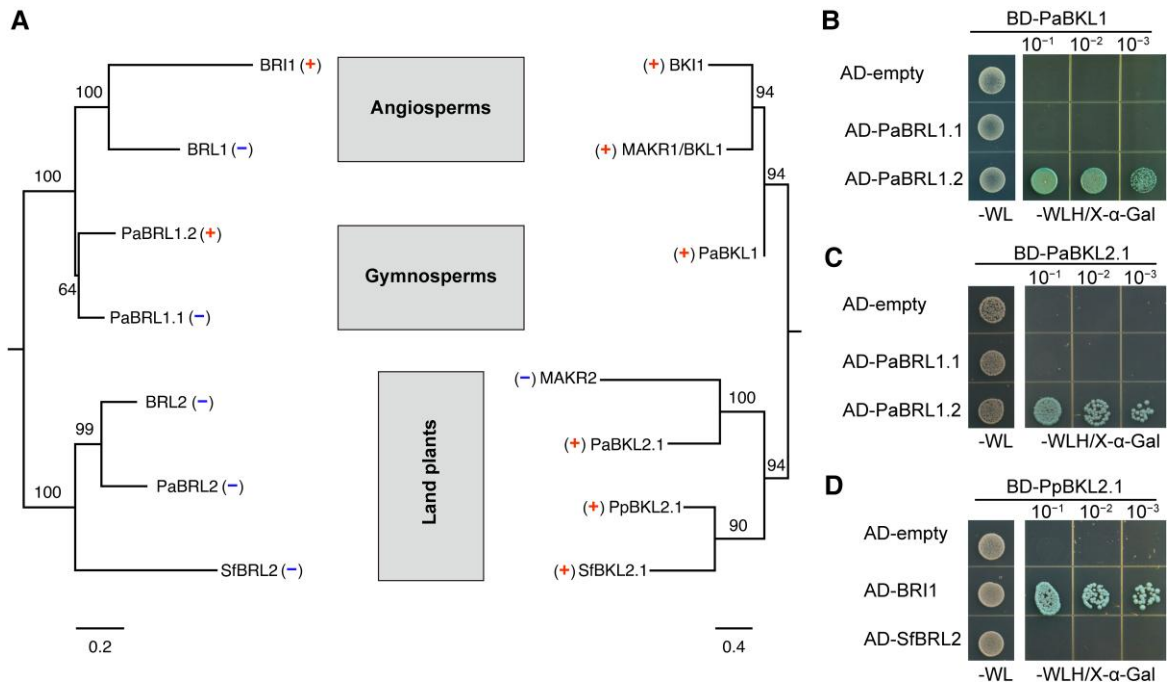
Figure 7 Functional associations of BKI1 and BRI1 families during plant evolution. A, Sharing phylogenetic trees (mirrortree) in BRI1 and BKI1 families. BRL2 and BKL2 originated in land plants, BRL1 and MAKRs/BKL1 originated in seed plants, and BRI1 and BKI1 coexisted in angiosperms. Presence (+) or absence (−) of an ability to interact is shown. The phylogenetic tree of BR receptors was built by the BD, a signature identified in BR receptors. The phylogenetic tree of the BKI1 family and MAKR2 that lost its ability to interact with BRI1 was built by the BIM. Support values were obtained from 1,000 bootstrap replicates. The scale bars indicate amino acid substitutions per site. B and C, PaBKL1 and PaBKL2.1 interacted with PaBRL1.2 but not PaBRL1.1 in yeast cells. D, PpBKL2.1 interacted with BRI1 but not SfBRL2 in yeast cells. Sf, *Sphagnum fallax*.

Supplemental Dataset 9). Furthermore, the acquisition of physical association is also an indication of coevolution (Ochoa et al., 2015). We found that the whole BKI1 family could interact with BRI1, but only angiosperm BRI1 and gymnosperm PaBRL1.2 (one copy of BRL1 in Pa) could interact with BKI1 family, while BRL2 and BRL1/PaBRL1.1 (the other copy of BRL1 in Pa) could not (Figure 7). This implies that PaBRL1.2 and BRI1 acquire a physical association with BKI1 family in gymnosperms and angiosperms after gene duplication, respectively. The question is whether their association is biologically relevant since functional dependency is an indication of coevolution as well. We showed that BKL2 could not inhibit transgenic Arabidopsis (Figures 4 and 5). Consistently, BRL2 and BKL2 were not always coexistent in liverworts, mosses, and lycophytes (Figure 7A and Supplemental Table 4). Furthermore, BKL2 did not present in gymnosperm Ginkgo and angiosperms (Supplemental Table 4). Conversely, BRL1 and MAKR1/BKL1 were always coexistent in gymnosperms, while BRI1 and BKI1 were always coexistent in angiosperms (Supplemental Table 4). Importantly, the physical association of BKI1 with BRI1 is required for the inhibitory function of BKI1 (Supplemental Figure 16). Furthermore, BKI1 had a stronger inhibitory function than MAKR1/BKL1 (Figures 4 and 5 and Supplemental Figure 4). Taken together, it is possible that BKL2 is essential in evolution but not in biological functions. Nevertheless, BRI1 and BKI1 families are likely coevolved, with the co-emergence of BKL2 and BRL2 in land plants, the co-option of MAKR1/BKL1 by BRL1 in seed plants, and the co-optimization of BKI1 and BRI1 in angiosperms.

Altogether, BKI1 family first acquires an ability to interact with BRI1 in the common ancestor of land plants (Figures 7 and 8, A and B). After a duplication event in seed plants, the new duplicate of BKL2 gains an ability to inhibit plant growth in its NT while elevating an ability to bind BRI1 in its CT, deriving MAKR1/BKL1 that weakly inhibits plant growth (Figure 8, A and B). After another duplication event in angiosperms, the new duplicate of MAKR1/BKL1 further gains an ability to inhibit plant growth in its NT and an ability to bind BRI1 in its CT, deriving BKI1 that strongly inhibits plant growth. Therefore, our results suggest that BKI1 family is neofunctionalized by a gain-of-function process in both their NT and CT by a seesaw mechanism (Figure 8C).

Discussion

Defining the BKI1 and MAKR families by their ability to interact with BRI1

BKI1/MAKRs regulate diverse functions in plant growth and development, yet knowledge about them has been limited to a few angiosperms (Wang and Chory, 2006; Jiang et al., 2015). Therefore, it is necessary to understand how BKI1/MAKRs acquire such a diverse function across the plant kingdom. A
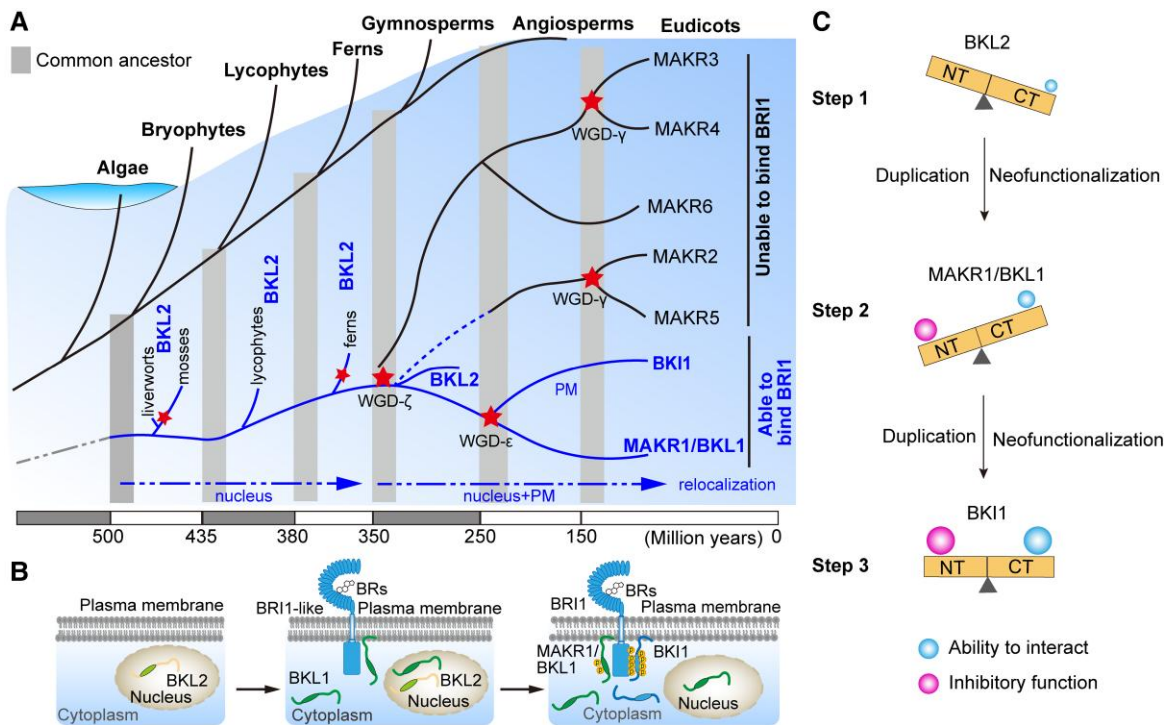
Figure 8 Model for the origin and functional evolution of the BKI1 and MAKR families. A, Origin and evolution of BKI1/MAKRs in land plants. The common ancestor of BKI1/MAKRs is able to interact with BRs receptors, which diverges into BKI1 family comprised of BKL2, BKL1, and BKI1 that can interact with BRI1 (family) and MAKR family composed of MAKR2-6 that cannot interact with BRI1 (family). By at least three WGD events, BKL2 presented in seedless plants; BKL1 and MAKR3/4 presented in seed plants; BKI1 and MAKR6 presented in angiosperms; and MAKR3, MAKR4, MAKR2, and MAKR5 diverged in dicots. B and C, The mechanism for the functional evolution of BKI1 family. During this process, BKI1 family members undergo subcellular relocalization from the nucleus to the PM (B) and further neofunctionalize by a stepwise "seesaw" model (C). A simple interpretation of this model is that BKL2 can interact with BRI1 at CT but with no inhibitory function at its NT. After a WGD event in seed plants, the ability to interact with BRI1 at CT of BKL1 is enhanced, which promotes the evolution in its NT, resulting in a gain of the inhibitory function at its NT. This radical change can generate negative feedback that prevents the CT from interacting with BRI1 (family). After another WGD event, a relaxation of this negative feedback in the extra duplicate is possible, allowing the CT to acquire the additional ability to interact with BRI1 (family). The enhanced ability to interact with BRI1 at CT of the extra duplicate can promote the evolution of its NT, resulting in a gain of the inhibitory function at its NT. As a result, the NT and CT of BKI1 can achieve a strong ability to interact and inhibit BRI1 (family) in angiosperms, generating compensatory coevolution between the ability to bind and the ability to inhibit BRI1 by a "seesaw" model.

large amount of the whole genome and transcriptome data provides an opportunity to investigate this problem. With BKI1 as the founder member, a previous study classifies BKI1/MAKR proteins into a family based on two conserved linear motifs within their sequences (Jaillais et al., 2011). Furthermore, functional analysis of these genes in *Arabidopsis* revealed that BKI1 has functional redundancy with only MAKR1 but not with any other MAKRs (Jaillais et al., 2011; Xuan et al., 2015; Kang and Hardtke, 2016; Marques-Bueno et al., 2021). We show that BKI1 presents across angiosperms while MAKR1 exists across seed plants. Hence, BKI1 is a derived putative paralog of MAKR1 (Figure 8A). Among all MAKRs found in Arabidopsis, only BKI1 and MAKR1 have the ability to interact and inhibit BRI1. Thus, MAKR1 originally coined by Jaillais is functionally a BKL, which we called BKL1, to differentiate those MAKRs that cannot interact and inhibit BRI1 (Jaillais et al., 2011). We also identified another previously unknown MAKR homolog from gymnosperms and seedless plants.

Interestingly, this MAKR homolog has the ability to interact with BRI1 but cannot inhibit BRI1. We thus named this MAKR as BKL2 and classified BKI1/MAKRs into BKI1 family able to interact with BRI1 and MAKR family unable to interact with BRI1 (Figure 8A).

Our extensive search across the plant kingdom has identified putative orthologs of BKL2 in seedless plants, MAKR3/4 (MAKR3), MAKR1/BKL1 together with BKL2 in gymnosperms, and MAKR2/5 (MAKR2), MAKR1/BKL1, BKI1, MAKR3/4 (MAKR3) together with MAKR6 in angiosperms (Figure 8A and Supplemental Figure 9). It is clear that MAKR6 is a duplicate of MAKR3/4 (MAKR3) in angiosperms (Figures 3 and 8A). The sudden loss of BKL2 is concomitant with the sudden emergence of MAKR2/5 (MAKR2) in angiosperms. Importantly, MAKR2/5 (MAKR2) is sister to gBKL2. Together, this permits us to propose that MAKR2/5 (MAKR2) is a loss-of-function BKL2 in angiosperms. It is conceivable that MAKR4 is a duplicate of MAKR3 while MAKR5 is a duplicate of MAKR2 emerged in dicots. Yet, there is no

MAKR in alga. Therefore, all MAKRs derive from a common ancestor shared with BKL2 in the common ancestor of land plants. Noticeably, this ancestor has an ability to interact with BRI1, which can then diverge into BKI1 family that can interact and inhibit BRI1 by a gain-of-function process and MAKR family that cannot interact and inhibit BRI1 by a loss-of-function process during seed plant evolution (Figure 8A), extremizing divergent evolution through their ability to interact with distinct protein partners (Kuriyan and Eisenberg, 2007).

Expansion of the BKI1 and MAKR families by WGDs

It has been reported that multiple rounds of WGD events occur during the evolution of land plants (One Thousand Plant Transcriptomes Initiative, 2019), which drives plant evolution (Jiao et al., 2011). During these events, many gene families were generated and expanded. In this study, we found that there was only one copy of BKL2 in *Marchantia polymorpha* (liverwort), and *S. moellendorffii* (lycophyte), but at least 3 copies in mosses (3 copies in Pp, 14 copies in *Sphagnum fallax* and 16 copies in *Sphagnum magellanicum*) and ferns (3 copies in *O. japonica*, 6 copies in *Ceratopteris richardii* and 7 copies in *Alsophila spinulosa*). This is consistent with the idea that the lineage-specific WGD events occur in mosses and ferns but not in the liverwort species (*M. polymorpha)* and lycophyte species (*S. moellendorffii*) (Figure 8A and Supplemental Figure 9) (Amborella Genome Project, 2013; Alix et al., 2017; Clark and Donoghue, 2018; One Thousand Plant Transcriptomes Initiative, 2019). Although the copy number of BKL2 increased in mosses and ferns, these copies of BKL2 clustered into a clade in the phylogenetic tree (Figure 3), indicating that they have limited functional diversification. Consistently, two copies of BKL2 in Pp interacted with BRI1, implying their redundancy (Figure 4A and Supplemental Figure 11A). Yet, BKL2 cannot inhibit plant growth when over-expressed (Figure 4, C–E and Supplemental Figure 11).

Previous studies have revealed that an ancient WGD event (WGD-ζ) occurred in the common ancestor of seed plants (Liu et al., 2022). Hence, three types of MAKRs in gymnosperms are grouped with three distinct angiosperm clades (Figure 3). One was grouped with the MAKR3/4 clade, and another was grouped with the BKI1/BKL1 clade, while the last one was sister to both BKI1/BKL1 and MAKR2/MAKR5 clades, implying that MAKR2/MAKR5 are a recent loss-of-function mutant of BKL2 in angiosperms (Figure 3). These results also suggest that an additional duplication arose from a WGD-ε event in the common ancestor of angiosperms. In addition, there were two copies of BKI1, MAKR1/BKL1, and MAKR3/4 in *Nymphaea colorata* (sister lineage to all extant angiosperms), but only one copy of them in *Amborella*, consistent with a lineage-specific WGD-π event occurred in *N. colorata* (Supplemental Figure 9) (Zhang, Berardini, et al., 2020; Zhang, Chen, et al., 2020). MAKR4 and MAKR5 were duplicates of MAKR3 and MAKR2 in dicots, respectively, generating four distinct copies, possibly as a consequence of the WGD-γ event (Figure 8A and Supplemental Figure 9 and Supplemental Dataset 10) (Amborella Genome Project, 2013; Xuan et al., 2015; Kang and Hardtke, 2016; Marques-Bueno et al., 2021). In this scenario, one of the two duplicates of MAKR6 is lost in dicots, resulting in only one copy of MAKR6 in dicots. Taken together, our analysis suggests that WGD events might be a major driver of the expansion of BKI1 and MAKR families. Yet, we are puzzling why there are three independent BKI1/MAKR clades instead of two in the common ancestor of seed plants since there is only one BKI1/MAKR clade in seedless plants (Figures 3 and 8A). Thus, it is possible that an unknown WGD event or even a non-WGD (lineage-specific duplication) event is involved in the evolution of BKI1/MAKRs in the common ancestor of seed plants, which requires further investigation.

Neofunctionalization of the BKI1 family by colocalization in the PM

Protein subcellular relocalization is an important molecular mechanism that contributes to the retention and neofunctionalization of duplicate genes (von der Dunk and Snel, 2020). In this study, we identified BKLs in different plant clades, and found that BKI1 was only present in angiosperms, MAKR1/BKL1 was only present in seed plants, and BKL2 was only present in gymnosperms and seedless plants. Although the BKL genes shared homology with BKI1, there were some striking differences in subcellular localization and therefore in their functions. We found that BKL2 was localized in the nucleus, and MAKR1/BKL1 was localized in the nucleus, cytoplasm and PM, whereas BKI1 was mainly localized in the PM (Figure 5E). These results suggest that the neofunctionalization of BKI1 family might accompany subcellular relocalization during evolution (Figure 8B).

Although most BKI1 family members can interact with BRI1-KD, only BKI1 and MAKR1/BKL1 can inhibit plant growth, but BKL2 cannot (Figures 4 and 7), suggesting that their functions are in part determined by their localization., Importantly, BRI1 is absent in seedless plants and gymnosperms (Wang and Chory, 2006; Ferreira-Guerra et al., 2020). However, there are two duplicates of BRI1/BRL1 (BRL1.1 and BRL1.2) in gymnosperms (Wang et al., 2021). Hence, it is possible that one acts as BRI1 while the other functions as BRL1. Consistently, PaBKL1 and PaBKL2.1 can interact with PaBRL1.2 but not PaBRL1.1, supporting our speculation (Figure 7, B and C). Furthermore, all BR receptors must localize to the PM to function (Friedrichsen et al., 2000; Wang et al., 2021). This suggests that colocalization of BKI1 with BRI1 and MAKR1/BKL1 with BRLs in angiosperms and gymnosperms, respectively, is possible. Following protein colocalization in cells, the local concentration of interacting partners can effectively increase, making coevolutionary events possible (Figure 8B) (Kuriyan and Eisenberg, 2007). In *Arabidopsis*, although the expression of *BKI1* and *MAKR1/BKL1* can inhibit plant growth via their interaction with BRI1, respectively, the inhibitory function of BKI1 is

much stronger than that of MAKR1/BKL1 in their transgenics (Supplemental Figure 4). Consistently, BKI1 can dissociate from PM by BR treatment, but MAKR1/BKL1 cannot (Jiang et al., 2015). These results are consistent with the idea that protein re-localization might lead to functional divergence of BKI1 and MAKR1/BKL1 in angiosperms, although the exact mechanism is unknown. Taken together, stepwise protein relocalization, at least in part, accelerates the neofunctionalization of BKI1 family during evolution (Figure 8B).

Neofunctionalization of the MAKR family by a loss of function in the BIM

MAKRs are a class of putative membrane-associated regulators that positively or negatively control plant growth and development (Jaillais et al., 2011). Their basic features necessary for the regulation of protein partners must be strictly constrained through their ability to interact with them. The BIM in their CT attracts interacting partners and therefore determines their specificity in the formation of MAKR complex (Wang and Chory, 2006; Jaillais et al., 2011). Although the exact role of the BIM in each specific member of the BKI1/MAKRs remains to be determined, this motif has been preserved for about 500 million years during land plant evolution (Morris et al., 2018). According to phylogenetic analysis and molecular dating, ancestral MAKR3/4 might have been derived in seed plants about 300 million years ago and further diverged into MAKR3 and MAKR4 in dicots about 119–125 million years ago (Figures 3 and 8A and Supplemental Figure 9) (Morris et al., 2018; Li et al., 2019; Liu et al., 2022). At the same time, ancestral MAKR2/5 was derived in angiosperms by a loss-of-function in BKL2 about 195–247 million years ago and further differentiated into MAKR2 and MAKR5 in dicots about 119–125 million years ago (Figures 3 and 7A and Supplemental Figure 9) (Morris et al., 2018; Li et al., 2019). MAKR6 was directly sister to MAKR3/4, likely derived from the common ancestor of angiosperms about 195–247 million years ago (Figures 3 and 8A and Supplemental Figure 9) (Morris et al., 2018; Li et al., 2019). Furthermore, we observed that the BIM was highly conserved within putative orthologs but diverged between putative paralogs, although they all shared six conserved residues in the BIM (Figure 3 and Supplemental Figure 1). Therefore, we propose that MAKR family might rapidly accumulate mutations in the BIM following gene duplication, which results in its loss of the ability to interact with BRI1.

Since the neofunctionalization model proposes that the new gene can add a new function without losing all the ancestral functions, MAKRs can be recognized after independent evolution for at least 100 millions of years. Finally, the advantageous mutations can be fixed in each MAKR by positive selection, leading to the neofunctionalization of the MAKR family (Figure 8A). Consistent with the Doll's law that loss-of-function evolution is not repeatable, we cannot reconstruct the function of MAKR3, so that they can inhibit plant growth (Figure 2 and Supplemental Figure 6),

supporting an aspect of unrepeatable evolution (Gould, 1970, 1989). Yet, we currently do not know why the ability to interact with BRI1 is beneficial for the ancestor of MAKR family but deleterious for MAKR family, thereby continuously losing it is beneficial for the expansion of MAKR family. We can only speculate that it might be governed by sign epistasis in which the same genotype can be beneficial in one background but deleterious in another background, presenting widespread compensatory mutations in MAKR family (Weinreich et al., 2005; Breen et al., 2012; Nghe et al., 2018; Storz, 2018; Rojas Echenique et al., 2019; Bakerlee et al., 2022).

Neofunctionalization model of the BKI1 family

Our findings allow us to propose a seesaw model for the evolution of BKI1 family (Figure 8C). In this model, the CT of the original duplicate first acquires the ability to interact with BRI1 (family), resulting in BKL2 with nuclear localization first. After the WGD-ζ event in seed plants, the ancestral BKL2 is duplicated to generate the ancestor of MAKR1/BKL1. This ancestor can colocalize with the ancestor of BRI1 family in the PM, which allosterically or/and epistatically promotes their coevolution, resulting in the acquisition of the ability to inhibit BRI1 in its NT. Therefore, a weaker functional MAKR1/BKL1 is derived from the extra duplicate of BKL2. In gymnosperms, ancestral gBKL1 (the extra duplicate of BKL2) would continuously but slowly evolve to become the extant gBKL1. In angiosperms, the common ancestor of MAKR1/BKL1 would be duplicated again in the common ancestor of angiosperms. After the WGD-ϵ event in angiosperms, the original duplicate would retain the ancestral function to become the extant MAKR1/BKL1, and the extra duplicate would be further neofunctionalized to become the extant BKI1. This duplication event can promote the evolution in the CT, which in turn further promotes the evolution in the NT. As such, the abilities to bind and to inhibit BRI1 can take turns to improve their functions in the NT and CT of BKI1 family during evolution, optimizing the function of BKI1 family by stepwise compensatory coevolution between the NT and the CT through a seesaw model (Figure 8C) (Farkas et al., 2022). Importantly, our proposed model can be partially recapitulated (Figures 5 and 6). Therefore, we uncover compensatory evolution by a seesaw model as an example of repeatable evolution, presenting an answer to the, Ohno's dilemma (Ohno, 1970; Bergthorsson et al., 2007).

Materials and methods

Phylogenetic analysis

Homologs of BKI1/MAKRs were retrieved from the Phytozome V13.0 (https://phytozome-next.jgi.doe.gov/), PhyloGenes (Zhang, Berardini, et al., 2020; Zhang, Chen, et al., 2020), Plantgenie (https://plantgenie.org/) databases, and (GIGA)^{n}DB (http://www.gigadb.org) (Sneddon et al.,

2012) using the protein sequence from Arabidopsis (Arabidopsis thaliana) as queries. The BLASTp searched the best-hit proteins as BKI1/MAKR homologs. Sequences were aligned using MAFFT (https://mafft.cbrc.jp/alignment/server/) with the L-INS-i strategy and other default parameters (Katoh and Standley, 2013). The sequences with long gaps were manually removed. Finally, we used the GUIDANCE2 webserver (http://guidance.tau.ac.il/) to create a super multiple sequence alignment (SuperMSA) by concatenating the default MSA and alternative 10 MSAs (Sela et al., 2015). All data sets were subjected to the ML approach using the W-IQ-TREE (http://iqtree.cibiv.univie.ac.at/) with default parameters, and the best-fitted evolutionary model was selected by auto model selection as implemented in IQ-TREE (Trifinopoulos et al., 2016). Branch support was tested with 1,000 replicates of Ultrafast (Hoang et al., 2018). Trees were visualized using Figtree (http://tree.bio.ed.ac.uk/software/FigTree/). The tree files and alignments were listed in Supplemental Datasets 1–7 and 10. Homologs of BRI1 were retrieved from the Phytozome V13.0 (https://phytozome-next.jgi.doe.gov/), and Plantgenie (https://plantgenie.org/). The BD (correspondent $BRI1^{580-673}$) was used to build the phylogenetic tree. A SuperMSA by concatenating the base MSA and 10 alternative MSAs computed by GUIDANCE2, a new integrated version of GUIDe tree based AligNment ConfidencE (GUIDANCE) algorithm, was used to construct the tree. Support values were obtained from 1,000 bootstrap replicates. The tree file and alignment were listed in Supplemental Dataset 9.

For sequence identity analysis, the protein sequences listed in Supplemental Dataset 8 were aligned using the MAFFT program, and sequence identity matrixes were performed by BioEdit v7.1.9 (http://www.mbio.ncsu.edu/bioedit/bioedit.html).

Yeast two-hybrid assays

To examine the interactions of BKI1 and MAKR1-6 with BR receptors, the full-length CDS of these genes were amplified from Col-0 cDNA and subcloned into pGBKT7 as bait. The intracellular domains of the BR receptors ($BRI1^{828-1196}$, $BRL1^{809-1166}$, $BRL2^{820-1143}$ from Arabidopsis thaliana and $PaBRL1.1^{888-1238}$, $PaBRL1.2^{894-1245}$ from Norway spruce [Pa]) were amplified from the genomic DNA of Col-0 and Pa, respectively, and then cloned into pGADT7 as prey. The intracellular domain of the BRL2 ($SfBRL2^{775-1085}$) from S. fallax was amplified from the genomic DNA and cloned into pGADT7. BKI1 homologs MAKR1/BKL1 and BKL2 from Pa, BKL2 from S. moellendorffii and Pp were amplified from cDNA and cloned into pGBKT7. Osmunda japonica BKL2 was synthesized by BGI. All constructs were identified by sequencing. Primers and constructs were listed in Supplemental Dataset 11. Bait and prey were co-transformed into Y2HGold and grown on SD medium lacking leucine and tryptophan to select for transformants. More than three colonies were used to evaluate the interactions on SD medium lacking leucine, tryptophan, and histidine.

Plant materials and genetic transformation

Arabidopsis thaliana ecotype Columbia (Col-0) was used as wild type. Seeds were germinated on ½ Murashige & Skoog (MS) medium after sterilization in 75% (v/v) ethanol for 10 min and then transferred to the soil. Plants were grown in the greenhouse under controlled conditions (16-h light/8-h dark cycles at 22°C–23°C). For phenotype analysis, images of seedlings or plants were taken at specified developmental stages.

To identify the effects of BKI1/MAKR genes on plant growth and development, the CDSs of these genes from representative species were amplified from bait constructs and cloned into pCHF3-GFP driven by BRI1 promoter (Zheng et al., 2019). In addition, the chimeric constructs of NT and CT replacement between BKI1 and MAKR3 were cloned into pCHF3-GFP driven by the MAKR3 promoter. The NT and CT chimeras between BKI1 and MAKR1/BKL1 were generated by overlapping PCR and subcloned into pCHF3-GFP driven by the BRI1 promoter. To detect the expression divergence of BKI1 and MAKR1/BKL1, we generated proBRI1:GUS, proBKI1:GUS, and proBKL1:GUS constructs. In short, 2 kb upstream fragments from ATG of BRI1, BKI1, and MAKR1/BKL1 were cloned from Col-0 DNA and then cloned into pCAMBIA-2300 vectors, respectively. To compare the functional differences, BKI1 and MAKR1/BKL1 under control of the 35S, BRI1, BKI1, and MAKR1/BKL1 promoters were then expressed in the plants, respectively. Primers and constructs were listed in Supplemental Dataset 11. All constructs were identified by sequencing. These constructs were transformed into Col-0 via the Agrobacterium tumefaciens (GV3101)-mediated floral dip method (Clough and Bent, 1998). Transgenic seeds were selected on ½ MS medium with kanamycin (50 mg/L). PCR genotypically verified each transgenic line, and the protein expression levels of transgenic lines were analyzed by immunoblotting.

GUS (the Escherichia coli β-glucuronidase gene uidA) staining

Plant tissues were fixed in precooled acetone for 30 min. The acetone was carefully discarded and then tissues vacuum infiltrated with 1–2 mL X-Gluc solution (50 mM potassium phosphate buffer pH 7.0, 0.5 mM ferrocyanide, 0.5 mM ferricyanide, 0.1% (v/v) Triton X-100, 0.5 mg/mL X-Gluc) for 10 min. After releasing the vacuum slowly, incubated tissues were placed in the staining solution at 37°C for 3 h. Chlorophyll was removed by washing tissues in 50% (v/v), 70% (v/v), and 90% (v/v) ethanol until the green tissue turned white.

Confocal microscopy

To observe the subcellular localization of BKI1 and BKLs, root tip cells of 4-day-old seedlings grown on ½ MS medium were used. The fluorescent signal of the reconstituted EGFP was imaged using a confocal laser scanning microscope (TCS SP8; Leica, Germany). The excitation wavelength for YFP was 488 nm. We collected the signals at 505–530 nm. Laser

intensity (10%) and detection settings (800 V Smart Gain) were kept constant. All confocal images under the objective lens (HC PL APO 40×/1.10 W CORR CS2) were exported as TIFF images with a single channel and merged into TIFF images with multiple channels.

Gene expression analysis

To determine the expression level of BR-responsive genes, we extracted the total RNA of 2-week-old seedlings by using a HiPure Plant RNA Mini Kit (Magen, #R4151-02). The first-strand cDNA was synthesized using 5× All-In-One RT MasterMix (abm, #G490), and cDNA was combined with ChamQ SYBR master mix for PCR (Vazyme, #Q311-02). The expression of BR responsive genes *CPD* (At5g05690), *DWF4* (At3g50660), *BAS1* (AT2G26710), and *Saur-AC1* (At4g38850) in Col-0, *BKI1*-overexpression, *MAKR1/BKL1*-overexpression, and *PaBKL1*-overexpression lines were detected by semi-quantitative reverse transcription polymerase chain reaction (RT-PCR). An *ACT2* gene (AT3G18780) was used as a control. Furthermore, the expression levels of *CPD* and *BAS1* in the above transgenic lines were confirmed using reverse transcription quantitative RT-PCR performed in triplicate with a Bio-Rad iCycler (Bio-Rad), and the data were collected with CFX96 Touch Real-Time PCR Detection System. The *ACT2* was used to normalize the data. All experiments were performed in triplicate. Primers were listed in Supplemental Dataset 11.

In vitro transphosphorylation assay

GST fusion constructs of the intracellular domain of BRI1$^{828-1196}$ and BRL2$^{809-1143}$ were generated by subcloning PCR products encoding the intracellular domains into the BamHI/SalI sites of pGEX-4T-3 (GST-containing vector). To detect the transphosphorylation of BKI1 and BKLs by BRI1$^{828-1196}$ and BRL2$^{809-1143}$, the GST-BKI1^{Cter} (BKI1$^{257-337}$), GST-BKL1^{Cter} (BKL1$^{264-341}$), GST-PaBKL1^{Cter} (PaBKL1$^{305-374}$), GST-OjBKL2 (OjBKL2$^{415-495}$), and GST-PpBKL2.1^{Cter} (PpBKL2.1$^{473-553}$) constructs were generated by subcloning PCR products encoding CT of BKI1 and BKLs into BamHI/SalI sites of pGEX-4T-3, respectively. Site-directed mutagenesis was used to create single-site and multiple-site mutations by overlapping PCR. Primers and constructs were listed in Supplemental Dataset 11. All constructs were identified by sequencing. The plasmids were transformed into *Escherichia coli* BL21 (DE3) cells and proteins were expressed overnight at 16°C and induced by the addition of 0.1 mM isopropyl-β-D-thiogalactoside. Proteins were purified via Glutathione Sepharose 4B purification followed by the manufacturer's instructions. GST-fusion proteins were added to the 20 μL reaction buffer (50 mM Tris-HCl, PH 7.4; 150 mM NaCl; 10 mM MgCl$_2$ and 10 mM ATP) at 37°C for 1 h. Reactions were terminated by adding 20 μL 2× SDS-PAGE (the SDS-PAGE method involves the denaturation of proteins with the detergent sodium dodecyl sulfate [SDS] and the use of an electric current to pull them through a polyacrylamide gel, a process termed polyacrylamide gel electrophoresis [PAGE])

loading buffer (62.5 mM Tris-HCl, PH 6.8, 2% (w/v) SDS, 10% (v/v) glycerol, 1% (v/v) β-mercaptoethanol, 0.005% (w/v) bromophenol blue) and boiling for 5 min at 100°C. Samples were separated on a 10% (w/v) SDS-PAGE Gel. Ponceau S staining determined protein transfer efficiency. The phosphorylation level was detected by immunoblotting with Phospho-Threonine Antibody (1:2,000 dilution, CST #9381), followed by a scan using Tanon Fine Do X6 automatic chemiluminescence image analysis system.

Immunoblot analysis

To detect the protein abundance of transgenic plants, total protein was extracted from 7-day-old seedlings of transgenic plants and Col-0 with 2× SDS loading buffer (62.5 mM Tris-HCl, PH 6.8, 2% (w/v) SDS, 10% (v/v) glycerol, 1% (v/v) β-mercaptoethanol, 0.005% (w/v) bromophenol blue), and boiling for 5 min at 95°C–100°C. Protein samples were separated on 10% (w/v) SDS–PAGE gels and transferred to nitrocellulose membranes (PALL Corporation, Cat#66485). The membranes were blocked with 5% (w/v) nonfat milk, rinsed with TBST and then incubated with primary and/or secondary antibodies. The primary antibodies used were anti-GFP (TransGen Biotech #HT801-01, 1:1,000), anti-Actin (Abmart #M20009, 1:1,000), and anti-Tubulin (Abmart #M20023, 1:2,000). The second antibodies used were Goat ant-Mouse IgG HRP (horseradish peroxidase) conjugate (Proteintech, #SA00001-1, 1:10,000) and Goat anti-Rabbit IgG HRP conjugate (Proteintech, #SA00001-2, 1:10,000). All antibodies were in 5% (w/v) nonfat milk in 1× TBST buffer. Chemiluminescence images were taken after adding Clarity Western enhanced chemiluminescence (ECL) substrate (Bio-Rad) with Tanon Fine Do X6.

To detect the phosphorylation status of BES1, total protein was extracted as described above, separated by 11% (w/v) Bis-Tris SDS-PAGE gel, and transferred onto the polyvinylidene difluoride membrane (PALL). The membrane was incubated with primary antibodies against BES1 (1:5,000, a gift from Jia Li, Lanzhou University, China) and then the corresponding HRP-conjugated secondary antibodies (anti-rabbit, 1:10,000). Chemiluminescence images were taken after adding Clarity Western ECL substrate (Bio-Rad) with Tanon Fine Do X6.

Rosette width, pedicel orientation, and hypocotyl analysis

Four-week-old plants were used for rosette width and leaf area analysis and 6-week-old plants were used for pedicel orientation analysis. Seedlings grown on ½ MS medium for five days under dark conditions were used for hypocotyl analysis. All data were measured by ImageJ software (Schindelin et al., 2012) and statistical analysis was performed by using one-way ANOVA and Tukey's multiple comparisons test as implemented in GraphPrism software (GraphPad Software, http://www.graphpad.com). Statistical analysis results are provided in Supplemental Dataset 12.

Accession numbers

Sequence data used in this work can be downloaded from TAIR (https://www.arabidopsis.org/), Phytozome 13 (https://phytozome.jgi.doe.gov/pz/portal.html#), PhyloGenes (Zhang, Berardini, et al., 2020; Zhang, Chen, et al., 2020), Plantgenie (https://plantgenie.org/) databases, and (GIGA)^{n}DB (http://gigadb.org/) (Sneddon et al., 2012). The genes used for experiments were listed under the following accession numbers and in Supplemental Dataset 1:

BRI1, AT4G39400; BRL1, AT1G55610; BRL2, AT2G01950; BKI1, AT5G42750; MAKR1/BKL1, AT5G26230; MAKR2, AT1G64080; MAKR3, AT2G37380; MAKR4, AT2G39370; MAKR5, AT5G52870; MAKR6, AT5G52900; PaBRL1.1, MA_57173; PaBRL1.2, MA_170; PaBKL1, MA_52346g; PaBKL2.1, MA_158390g; PaBKL2.2, MA_10136386g; OjBKL2, c8891_g1_i1; SmBKL2, 412582; PpBKL2.1, Pp3c7_4510; PpBKL2.2, Pp3c11_22260; SfBRL2 (Sphfalx07G109200).

Supplemental Data

The following materials are available in the online version of this article.

Supplemental Figure S1. The conserved BRI1-interacting motif of BKI1/MAKRs in representative species.

Supplemental Figure S2. The phylogenetic tree of full-length BKI1/MAKRs in angiosperms.

Supplemental Figure S3. The phylogenetic tree of the N-terminus (NT) of BKI1/MAKRs in angiosperms.

Supplemental Figure S4. MAKR1/BKL1 has a weaker inhibitory function than BKI1 in transgenic Arabidopsis.

Supplemental Figure S5. Like BKI1, MAKR1/BKL1 and PaBKL1 are involved in BR signaling.

Supplemental Figure S6. Unexchangeable function in both N-terminus and C-terminus of Arabidopsis BKI1 and MAKR3.

Supplemental Figure S7. Phylogenetic tree of plant BKI1/MAKRs in the plant kingdom.

Supplemental Figure S8. Phylogenetic tree of the N-termini (NTs) of BKI1/MAKRs in the plant kingdom.

Supplemental Figure S9. Phylogenetic profile of BKI1/MAKRs in the plant kingdom.

Supplemental Figure S10. Protein sequence alignment of MAKR1/BKL1 and BKL2 from *Picea abies*.

Supplemental Figure S11. Analysis of the ability to bind and inhibit BRI1 by BKLs.

Supplemental Figure S12. C-terminal domain of BKI1 family used for transphosphorylation analysis.

Supplemental Figure S13. Sequence and interaction analysis of putative MAKR3/4 orthologs in *Picea abies*.

Supplemental Figure S14. Schematic representation of the N- and C-terminus replacement between BKI1 and BKLs.

Supplemental Figure S15. Multiple sequence alignments of BKI1 and BKLs and identification of [KR] motifs.

Supplemental Figure S16. Physical association of BKI1 with BRI1 via BKI1-BIM was required for growth inhibition in the transgenic plants of BKI1.

Supplemental Table S1. Nomenclatures of BKI1, MAKR, and BRI1 families with their original names highlighted.

Supplemental Table S2. Sequence identity analysis of the putative orthologs of MAKR1/BKL1 in gymnosperms.

Supplemental Table S3. Identity analysis of MAKR1/BKL1, BKL2, and MAKR3/4 in *Picea abies*.

Supplemental Table S4. Distribution of the members of BKI1 and BRI1 families in selective species of land plants.

Supplemental Dataset S1. Gene information used in this work.

Supplemental Dataset S2. The tree file and alignment of protein sequences used to generate the phylogenetic tree in Figure 1.

Supplemental Dataset S3. The tree file and alignment of protein sequences used to generate the phylogenetic tree in Figure S2.

Supplemental Dataset S4. The tree file and alignment of protein sequences used to generate the phylogenetic tree in Figure S3.

Supplemental Dataset S5. The tree file and alignment of protein sequences used to generate the phylogenetic tree in Figure 3.

Supplemental Dataset S6. The tree file and alignment of protein sequences used to generate the phylogenetic tree in Figure S7.

Supplemental Dataset S7. The tree file and alignment of protein sequences used to generate the phylogenetic tree in Supplemental Figure S8.

Supplemental Dataset S8. Sequences used for identity analysis .

Supplemental Dataset S9. The tree file and alignment of protein sequences used to generate the phylogenetic tree in Figure 7.

Supplemental Dataset S10. The tree files and alignments of protein sequences used to generate the phylogenetic tree in Supplemental Figure S9.

Supplemental Dataset S11. Primers and constructs used in this work.

Supplemental Dataset S12. Summary of statistical tests.

Acknowledgments

Funding

References

Amborella Genome Project (2013) The Amborella genome and the evolution of flowering plants. Science **342**(6165): 1241089

One Thousand Plant Transcriptomes Initiative (2019) One thousand plant transcriptomes and the phylogenomics of green plants. Nature **574**(7780): 679–685

Alix K, Gerard PR, Schwarzacher T, Heslop-Harrison JSP (2017) Polyploidy and interspecific hybridization: partners for adaptation, speciation and evolution in plants. Ann Bot **120**(2): 183–194

Bakerlee CW, Nguyen Ba AN, Shulgina Y, Rojas Echenique JI, Desai MM (2022) Idiosyncratic epistasis leads to global fitness-correlated trends. Science **376**(6593): 630–635

Bergthorsson U, Andersson DI, Roth JR (2007) Ohno's dilemma: evolution of new genes under continuous selection. Proc Natl Acad Sci U S A **104**(43): 17004–17009

Birchler JA, Yang H (2022) The multiple fates of gene duplications: deletion, hypofunctionalization, subfunctionalization, neofunctionalization, dosage balance constraints, and neutral variation. Plant Cell **34**(7): 2466–2474

Bowman JL, Kohchi T, Yamato KT, Jenkins J, Shu S, Ishizaki K, Yamaoka S, Nishihama R, Nakamura Y, Berger F, et al. (2017) Insights into land plant evolution garnered from the *Marchantia polymorpha* genome. Cell **171**(2): 287–304.e15

Breen MS, Kemena C, Vlasov PK, Notredame C, Kondrashov FA (2012) Epistasis as the primary factor in molecular evolution. Nature **490**(7421): 535–538

Cano-Delgado A, Yin Y, Yu C, Vafeados D, Mora-Garcia S, Cheng JC, Nam KH, Li J, Chory J (2004) BRL1 and BRL3 are novel brassinosteroid receptors that function in vascular differentiation in Arabidopsis. Development **131**(21): 5341–5351

Clark JW, Donoghue PCJ (2018) Whole-genome duplication and plant macroevolution. Trends Plant Sci **23**(10): 933–945

Clough SJ, Bent AF (1998) Floral dip: a simplified method for Agrobacterium-mediated transformation of *Arabidopsis thaliana*. Plant J **16**(6): 735–743

de Juan D, Pazos F, Valencia A (2013) Emerging methods in protein co-evolution. Nat Rev Genet **14**(4): 249–261

Dievart A, Gottin C, Perin C, Ranwez V, Chantret N (2020) Origin and diversity of plant receptor-like kinases. Annu Rev Plant Biol **71**(1): 131–156

Diss G, Gagnon-Arsenault I, Dion-Cote AM, Vignaud H, Ascencio DI, Berger CM, Landry CR (2017) Gene duplication can impart fragility, not robustness, in the yeast protein interaction network. Science **355**(6325): 630–634

Fabregas N, Li N, Boeren S, Nash TE, Goshe MB, Clouse SD, de Vries S, Cano-Delgado AI (2013) The brassinosteroid insensitive1-like3 signalosome complex regulates *Arabidopsis* root development. Plant Cell **25**(9): 3377–3388

Farkas Z, Kovacs K, Sarkadi Z, Kalapis D, Fekete G, Birtyik F, Ayaydin F, Molnar C, Horvath P, Pal C, et al. (2022) Gene loss and

compensatory evolution promotes the emergence of morphological novelties in budding yeast. Nat Ecol Evol **6**(6): 763–773

Ferreira-Guerra M, Marques-Bueno M, Mora-Garcia S, Cano-Delgado AI (2020) Delving into the evolutionary origin of steroid sensing in plants. Curr Opin Plant Biol **57**: 87–95

Flagel LE, Wendel JF (2009) Gene duplication and evolutionary novelty in plants. New Phytol **183**(3): 557–564

Force A, Lynch M, Pickett FB, Amores A, Yan YL, Postlethwait J (1999) Preservation of duplicate genes by complementary, degenerative mutations. Genetics **151**(4): 1531–1545

Friedrichsen DM, Joazeiro CA, Li J, Hunter T, Chory J (2000) Brassinosteroid-insensitive-1 is a ubiquitously expressed leucine-rich repeat receptor serine/threonine kinase. Plant Physiol **123**(4): 1247–1256

Furumizu C, Sawa S (2021) Insight into early diversification of leucine-rich repeat receptor-like kinases provided by the sequenced moss and hornwort genomes. Plant Mol Biol **107**(4-5): 337–353

Gibson TA, Goldberg DS (2009) Questioning the ubiquity of neofunctionalization. PLoS Comput Biol **5**(1): e1000252

Gou X, He K, Yang H, Yuan T, Lin H, Clouse SD, Li J (2010) Genome-wide cloning and sequence analysis of leucine-rich repeat receptor-like protein kinase genes in Arabidopsis thaliana. BMC Genomics **11**(1): 19

Gould SJ (1970) Dollo on Dollo's Law: irreversibility and the status of evolutionary laws. J Hist Biol **3**(2): 189–212

Gould SJ (1989) Wonderful Life. W.W. Norton, New York, pp 1–347

Hallin J, Landry CR (2019) Regulation plays a multifaceted role in the retention of gene duplicates. PLoS Biol **17**(11): e3000519

He X, Zhang J (2005) Rapid subfunctionalization accompanied by prolonged and substantial neofunctionalization in duplicate gene evolution. Genetics **169**(2): 1157–1164

Hoang DT, Chernomor O, von Haeseler A, Minh BQ, Vinh LS (2018) UFBoot2: improving the ultrafast bootstrap approximation. Mol Biol Evol **35**(2): 518–522

Hughes AL (1994) The evolution of functionally novel proteins after gene duplication. Proc Biol Sci **256**(1346): 119–124

Innan H, Kondrashov F (2010) The evolution of gene duplications: classifying and distinguishing between models. Nat Rev Genet **11**(2): 97–108

Jaillais Y, Hothorn M, Belkhadir Y, Dabi T, Nimchuk ZL, Meyerowitz EM, Chory J (2011) Tyrosine phosphorylation controls brassinosteroid receptor activation by triggering membrane release of its kinase inhibitor. Genes Dev **25**(3): 232–237

Jiang J, Wang T, Wu Z, Wang J, Zhang C, Wang H, Wang Z-X, Wang X (2015) The intrinsically disordered protein BKI1 is essential for inhibiting BRI1 signaling in plants. Mol Plant **8**(11): 1675–1678

Jiao Y, Wickett NJ, Ayyampalayam S, Chanderbali AS, Landherr L, Ralph PE, Tomsho LP, Hu Y, Liang H, Soltis PS, et al. (2011) Ancestral polyploidy in seed plants and angiosperms. Nature **473**(7345): 97–100

Kang YH, Hardtke CS (2016) Arabidopsis MAKR5 is a positive effector of BAM3-dependent CLE45 signaling. EMBO Rep **17**(8): 1145–1154

Katoh K, Standley DM (2013) MAFFT multiple sequence alignment software version 7: improvements in performance and usability. Mol Biol Evol **30**(4): 772–780

Kinoshita T, Cano-Delgado A, Seto H, Hiranuma S, Fujioka S, Yoshida S, Chory J (2005) Binding of brassinosteroids to the extracellular domain of plant receptor kinase BRI1. Nature **433**(7022): 167–171

Kiryakova Y, Padula M, Rossano R, Martelli G (2016) Effect of boron and zinc application on HXK1 and MAKR6 gene expression in strawberry. Emirates J Food Agric **28**(5): 317–325

Kuriyan J, Eisenberg D (2007) The origin of protein interactions and allostery in colocalization. Nature **450**(7172): 983–990

Li J, Chory J (1997) A putative leucine-rich repeat receptor kinase involved in brassinosteroid signal transduction. Cell **90**(5): 929–938

Li HT, Yi TS, Gao LM, Ma PF, Zhang T, Yang JB, Gitzendanner MA, Fritsch PW, Cai J, Luo Y, et al. (2019) Origin of angiosperms and the puzzle of the Jurassic gap. Nat Plants **5**(5): 461–470

Liu Y, Wang S, Li L, Yang T, Dong S, Wei T, Wu S, Liu Y, Gong Y, Feng X, et al. (2022) The Cycas genome and the early evolution of seed plants. Nat Plants **8**(4): 389–401

Liu H, Wang X, Wang G, Cui P, Wu S, Ai C, Hu N, Li A, He B, Shao X, et al. (2021) The nearly complete genome of *Ginkgo biloba* illuminates gymnosperm evolution. Nat Plants **7**(6): 748–756

Lynch M, Conery JS (2000) The evolutionary fate and consequences of duplicate genes. Science **290**(5494): 1151–1155

Magadum S, Banerjee U, Murugan P, Gangapur D, Ravikesavan R (2013) Gene duplication as a major force in evolution. J Genet **92**(1): 155–161

Marques-Bueno MM, Armengot L, Noack LC, Bareille J, Rodriguez L, Platre MP, Bayle V, Liu M, Opdenacker D, Vanneste S, et al. (2021) Auxin-regulated reversible inhibition of TMK1 signaling by MAKR2 modulates the dynamics of root gravitropism. Curr Biol **31**(1): 228–237.e10

Morris JL, Puttick MN, Clark JW, Edwards D, Kenrick P, Pressel S, Wellman CH, Yang Z, Schneider H, Donoghue PCJ (2018) The timescale of early land plant evolution. Proc Natl Acad Sci U S A **115-**(10): E2274–E2283

Neben CL, Lo M, Jura N, Klein OD (2019) Feedback regulation of RTK signaling in development. Dev Biol **447**(1): 71–89

Nghe P, Kogenaru M, Tans SJ (2018) Sign epistasis caused by hierarchy within signalling cascades. Nat Commun **9**(1): 1451

Novikova DD, Korosteleva AL, Mironova V, Jaillais Y (2021) Meet your MAKR: the membrane-associated kinase regulator protein family in the regulation of plant development. FEBS J **289**(20): 6172–6186

Nystedt B, Street NR, Wetterbom A, Zuccolo A, Lin YC, Scofield DG, Vezzi F, Delhomme N, Giacomello S, Alexeyenko A, et al. (2013) The Norway spruce genome sequence and conifer genome evolution. Nature **497**(7451): 579–584

Ochoa D, Juan D, Valencia A, Pazos F (2015) Detection of significant protein coevolution. Bioinformatics **31**(13): 2166–2173

Ohno S (1970) Evolution by Gene Duplication. Springer-Verlag, New York, USA, pp 59–89

Panchy N, Lehti-Shiu M, Shiu SH (2016) Evolution of gene duplication in plants. Plant Physiol **171**(4): 2294–2316

Qiu Y, Tay YV, Ruan Y, Adams KL (2020) Divergence of duplicated genes by repeated partitioning of splice forms and subcellular localization. New Phytol **225**(2): 1011–1022

Rastogi S, Liberles DA (2005) Subfunctionalization of duplicated genes as a transition state to neofunctionalization. BMC Evol Biol **5**(1): 28

Ren L-L, Liu Y-J, Liu H-J, Qian T-T, Qi L-W, Wang X-R, Zeng Q-Y (2014) Subcellular relocalization and positive selection play key roles in the retention of duplicate genes of populus class III peroxidase family. Plant Cell **26**(6): 2404–2419

Rojas Echenique JI, Kryazhimskiy S, Nguyen Ba AN, Desai MM (2019) Modular epistasis and the compensatory evolution of gene deletion mutants. PLoS Genet **15**(2): e1007958

Schindelin J, Arganda-Carreras I, Frise E, Kaynig V, Longair M, Pietzsch T, Preibisch S, Rueden C, Saalfeld S, Schmid B, et al. (2012) Fiji: an open-source platform for biological-image analysis. Nat Methods **9**(7): 676–682

Sela I, Ashkenazy H, Katoh K, Pupko T (2015) GUIDANCE2: accurate detection of unreliable alignment regions accounting for the uncertainty of multiple parameters. Nucleic Acids Res **43**(W1): W7–W14

Shiu SH, Bleecker AB (2001) Receptor-like kinases from Arabidopsis form a monophyletic gene family related to animal receptor kinases. Proc Natl Acad Sci U S A **98**(19): 10763–10768

Sneddon TP, Li P, Edmunds SC (2012) GigaDB: announcing the GigaScience database. Gigascience **1**(1): 11

Storz JF (2018) Compensatory mutations and epistasis for protein function. Curr Opin Struct Biol **50**: 18–25

Trifinopoulos J, Nguyen LT, von Haeseler A, Minh BQ (2016) W-IQ-TREE: a fast online phylogenetic tool for maximum likelihood analysis. Nucleic Acids Res **44**(W1): W232–W235

von der Dunk SHA, Snel B (2020) Recurrent sequence evolution after independent gene duplication. BMC Evol Biol **20**(1): 98

Wang X, Chory J (2006) Brassinosteroids regulate dissociation of BKI1, a negative regulator of BRI1 signaling, from the plasma membrane. Science **313**(5790): 1118–1122

Wang J, Jiang J, Wang J, Chen L, Fan S-L, Wu J-W, Wang X, Wang Z-X (2014) Structural insights into the negative regulation of BRI1 signaling by BRI1-interacting protein BKI1. Cell Res **24**(11): 1328–1341

Wang L, Liu J, Shen Y, Pu R, Hou M, Wei Q, Zhang X, Li G, Ren H, Wu G (2021) Brassinosteroids synthesised by CYP85A/A1 but not CYP85A2 function via a BRI1-like receptor but not via BRI1 in *Picea abies*. J Exp Bot **72**(5): 1748–1763

Wang ZY, Seto H, Fujioka S, Yoshida S, Chory J (2001) BRI1 is a critical component of a plasma-membrane receptor for plant steroids. Nature **410**(6826): 380–383

Wang D, Yang C, Wang H, Wu Z, Jiang J, Liu J, He Z, Chang F, Ma H, Wang X (2017) BKI1 Regulates plant architecture through coordinated inhibition of the brassinosteroid and ERECTA signaling pathways in Arabidopsis. Mol Plant **10**(2): 297–308

Wang H, Yang C, Zhang C, Wang N, Lu D, Wang J, Zhang S, Wang Z-X, Ma H, Wang X (2011) Dual role of BKI1 and 14-3-3 s in brassinosteroid signaling to link receptor with transcription factors. Dev Cell **21**(5): 825–834

Weinreich DM, Watson RA, Chao L (2005) Perspective: sign epistasis and genetic constraint on evolutionary trajectories. Evolution **59**(6): 1165–1174

Xuan W, Audenaert D, Parizot B, Moller BK, Njo MF, De Rybel B, De Rop G, Van Isterdael G, Mahonen AP, Vanneste S, et al. (2015) Root cap-derived auxin pre-patterns the longitudinal axis of the Arabidopsis root. Curr Biol **25**(10): 1381–1388

Zhang P, Berardini TZ, Ebert D, Li Q, Mi H, Muruganujan A, Prithvi T, Reiser L, Sawant S, Thomas PD, et al. (2020) Phylogenes: an online phylogenetics and functional genomics resource for plant gene function inference. Plant Direct **4**(12): e00293

Zhang L, Chen F, Zhang X, Li Z, Zhao Y, Lohaus R, Chang X, Dong W, Ho SYW, Liu X, et al. (2020) The water lily genome and the early evolution of flowering plants. Nature **577**(7788): 79–84

Zheng B, Bai Q, Wu L, Liu H, Liu Y, Xu W, Li G, Ren H, She X, Wu G (2019) EMS1 and BRI1 control separate biological processes via extracellular domain diversity and intracellular domain conservation. Nat Commun **10**(1): 4165

Zhou A, Wang H, Walker JC, Li J (2004) BRL1, a leucine-rich repeat receptor-like protein kinase, is functionally redundant with BRI1 in regulating Arabidopsis brassinosteroid signaling. Plant J **40**(3): 399–409